Title: High contribution of anthropogenic combustion sources to atmospheric inorganic reactive nitrogen in South China evidenced by isotopes

Manuscript ID: acp-2023-49

Dear editor:

Thank you for your letter.

We appreciate the two referees for their professional comments on our manuscript. We considered these detailed comments and responded to their suggestions and questions. Based on referees' comments, we have carefully revised our manuscript. The following is one-on-one response to the reviewers for your reference. Revised texts are marked in red in our manuscript.

We sincerely appreciate your consideration. If there are any questions, please contact us. We will do our best to solve it.

With Best Regards,

Jun Li

junli@gig.ac.cn

Response to Referee #1

RC- Reviewer's Comments; AC – Authors' Response Comments

RC1: The manuscript by Li et al. simultaneously reported concentrations and stable nitrogen isotope and oxygen isotopes compositions of atmospheric NO_3^- and concentrations and nitrogen isotopes compositions of atmospheric NH_4^+ in $PM_{2.5}$ samples collected in Guangzhou from May 2017 to June 2018. Then, authors restrained nitrogen isotope fractionation values of the process of NH_3 to formed NH_4^+ and NO_x to formed NO_3^-. Finally, using the IsoSource model, authors quantified the relative contributions of major sources of NH_3 and NO_x to atmospheric NH_4^+ and NO_3^-, respectively. Authors found the focus of NH_3 reduction should be on anthropogenic combustion sources especially on biomass burning, which might be responsible for the lag of the decline in deposition of air pollutions behind the reduction in emission. Additionally, despite a series of measures to reduce emissions of NO_x, fossil fuels, as the main energy for production and living, will still inevitably emit a large amount of NO_x. Authors emphasized that the emission of atmospheric inorganic nitrogen is largely related to anthropogenic combustion sources. The development and promotion of clean energy and efficient use of biomass are conducive to the deep reduction of atmospheric nitrogen. I believe that this result is meaningful and would make a substantial contribution to the field. The manuscript is generally well-organized in structure. If the following comments are adequately addressed, I believe the manuscript could be accepted to Atmospheric Chemistry and Physics.

AC1: We appreciate your constructive comments and professional suggestions. These comments and suggestions are helpful for improving our manuscript. Based on your comments and suggestions, we have revised our manuscript. If you have any further comments and suggestions, we will do our best to improve our manuscript.

We would like to show the details as follows:

RC2: Lines 112-113: The author needs to provide the analytical accuracy of isotopes nitrogen and oxygen isotopes.

AC2: Thanks for your suggestion. We have added details on the accuracy of nitrogen and oxygen isotope analysis, as shown in the marked revised manuscript **lines 120-127**: To ensure the stability of the instrument, standard samples were tested for every ten samples. The standard deviation of replicates was generally less than 0.4‰, 0.8‰, and 0.5‰ for $\delta^{15}N\text{-}NO_3^-$, $\delta^{18}O\text{-}NO_3^-$, and $\delta^{15}N\text{-}NH_4^+$, respectively. The instrumental values of $\delta^{15}N\text{-}NO_3^-$ and $\delta^{18}O\text{-}NO_3^-$ were corrected by multi-point correction ($\delta^{18}O$ r^2=0.99, $\delta^{15}N$ r^2=0.999) based on international standards (IAEA-NO-3, USGS32, USGS34, and USGS35). The measured values of $\delta^{15}N\text{-}NH_4^+$ were also corrected by multi-point correction (r^2=0.999) based on international standards (IAEA-N1, USGS25, and USGS26).

RC3: Nitrogen isotope fractionation values of the process of NH_3 to formed NH_4^+ and NOx to formed NO_3^- are key parameters for quantifying the relative contributions of major sources of NH_3 and NOx to atmospheric NH_4^+ and NO_3^-. The calculation methods for the two parameters should be include in the text of manuscript. In addition, it is necessary to give readers detailed data of each parameter, especially the fractionation value.

AC3: Thanks for your professional comment and kind suggestion.

a. Nitrogen isotope fractionation values of the process of NH_3 to form NH_4^+.

Atmospheric initial $\delta^{15}N\text{-}NH_3$ was calculated by following equation 1.

$$\delta^{15}N\text{-}NH_{3\text{-initial}} = \delta^{15}N\text{-}NH_4^+ - \varepsilon(NH_4^+\text{-}NH_3) \times (1 - f) \quad (1)$$

Where, $\delta^{15}N\text{-}NH_4^+$ and $\delta^{15}N\text{-}NH_{3\text{-initial}}$ represent the $\delta^{15}N$ of particulate NH_4^+ and atmospheric initial NH_3, respectively. $\varepsilon(NH_4^+\text{-}NH_3)$ represents the isotope fractionation factor in the gaseous NH_3 conversion to particulate NH_4^+ in the atmosphere. The f value represents the proportion of the initial NH_3 converted to NH_4^+, referring to NH_3 and NH_4^+ observed in Guangzhou (Liao et al., 2014).

The $\varepsilon(NH_4^+\text{-}NH_3)$ value is temperature dependent(Huang et al., 2019), which can

be deduced from(Urey, 1947), as shown in equation 2. The atmospheric average temperature was 24.5℃ in our sampling period, and the corresponding $\varepsilon(NH_4^+\text{-}NH_3)$ value was 34.2‰ calculated by equation 2. In addition, the $\varepsilon(NH_4^+\text{-}NH_3)$ in Guangzhou was estimated to be 32.4‰ according to equation 6. Equation 6 was deduced by equations 3-5. According to equation 6, a linear fitting equation was observed between fNH_4^+ and $\delta^{15}N\text{-}NH_4^+$ (**Referee#1_Figure 1**), and the absolute value of the slope (32.4‰) was equal to $\varepsilon(NH_4^+\text{-}NH_3)$. The $\varepsilon(NH_4^+\text{-}NH_3)$ average of the two methods (34.2‰ and 32.4‰) was 33.3‰ and approximated to the experimental isotope enrichment factor (33‰)(Heaton et al., 1997). Therefore, +33‰ was used for deducing the $\delta^{15}N$ of the initial NH_3. We have added the calculation process to manuscript. Please see **lines 137-162** in the marked revised manuscript.

$$\varepsilon_{(NH_4^+\_NH_3)} = 12.4678 * \frac{1000}{T+273.15} - 7.6694 \quad (2)$$

$$\delta^{15}N\text{-}NH_4^+ - \delta^{15}N\text{-}NH_3 = \varepsilon_{(NH_4^+\_NH_3)} \quad (3)$$

$$fNH_4^+ + fNH_3 = 1 \quad (4)$$

$$\delta^{15}N\text{-}NH_4^+ * fNH_4^+ + \left(\delta^{15}N\text{-}NH_4^+ - \varepsilon_{(NH_4^+\_NH_3)}\right) * (1 - fNH_4^+) = \delta^{15}N \quad (5)$$

$$\delta^{15}N\text{-}NH_4^+ = -\varepsilon_{(NH_4^+\_NH_3)} * fNH_4^+ + (\delta^{15}N + \varepsilon_{(NH_4^+\_NH_3)}) \quad (6)$$

Where, T represents the atmospheric temperature (℃). $\delta^{15}N\text{-}NH_4^+$ and $\delta^{15}N\text{-}NH_3$ represent the $\delta^{15}N$ of particulate NH_4^+ and atmospheric NH_3, respectively. $\delta^{15}N$ represents the sum of $\delta^{15}N\text{-}NH_4^+$ and $\delta^{15}N\text{-}NH_3$. fNH_3 and fNH_4^+ represent the proportion of atmospheric NH_3 and particulate NH_4^+, respectively.

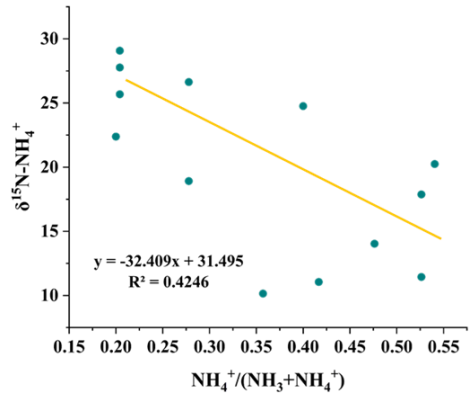

Referee#1_Figure 1 (Figure S1 in SI). Linear fitting of $NH_4^+/(NH_3+NH_4^+)$ with $\delta^{15}N$-

NH_4^+.

b. Nitrogen isotope fractionation values of the process of NO_x to form NO_3^-

In Central Pearl River Delta, NO_3^- formed through ·OH and N_2O_5 pathways contributed to 94% simulated by CAMQ model (Qu et al., 2021). In this study, only ·OH (R4) and N_2O_5 (R5-R7) formation pathways were considered. The reasons why we only consider the ·OH oxidation and N_2O_5 hydrolysis pathway to form NO_3^- were explained in detail in the **AC7**.

$NO + O_3 \rightarrow NO_2 + O_2$ (R1)

$NO_2 + hv \rightarrow NO + O$ (R2)

$O + O_2 \rightarrow O_3$ (R3)

$NO_2 + \cdot OH \rightarrow HNO_3$ (R4)

$NO_2 + O_3 \rightarrow NO_3 + O_2$ (R5)

$NO_2 + NO_3 \rightarrow N_2O_5$ (R6)

$N_2O_5 + H_2O \rightarrow 2HNO_3$ (R7)

$HNO_3 + Alkali \rightarrow NO_3^-$ (R8)

The specific details of the Bayesian mixing model were reported by our previous studies (Zong et al., 2017; Zong et al., 2020). The principle and process of Bayesian mixing model was shown in **Referee#1_Figure 2** adapted from Zong et al., (Zong et al., 2017). The atmospheric $\delta^{18}O\text{-}NO_3^-$ can be expressed by equation 7. The $[\delta^{18}O\text{-}HNO_3]_{OH}$ can be further expressed by equation 8 assuming no kinetic isotope fractionation (Walters and Michalski, 2016). And $[\delta^{18}O\text{-}HNO_3]_{H2O}$ can be estimated by equation 9 (Walters and Michalski, 2016). The $\delta^{18}O$ values in tropospheric H_2O, NOx, O_3, and OH were within a certain range. The tropospheric $\delta^{18}O\text{-}H_2O$, $\delta^{18}O\text{-}NOx$, $\delta^{18}O\text{-}O_3$, and $\delta^{18}O\text{-}OH$ ranged from -25‰ to 0‰(Baskaran et al., 2011; Walters and Michalski, 2016), 112‰ to 122‰ (Michalski et al., 2014; Walters and Michalski, 2016), 90‰ to 122‰, and -15‰ to 0‰, respectively(Fang et al., 2011; Johnston and Thiemens, 1997). Therefore, the γ (the contribution of ·OH formation pathway) can be estimated by fNO_2 and oxygen isotope fractionation i.e., $\alpha NO_2/NO$, $\alpha OH/H_2O$, and $\alpha N_2O_5/NO_2$. The oxygen isotope fractionations are temperature dependent and can be estimated by equation 11. The fNO_2 varied from 0.20 to 0.95(Zong et al., 2017; Walters et al., 2016).

Based on $\delta^{18}O\text{-}NO_3^-$, $\delta^{18}O\text{-}H_2O$, $\delta^{18}O\text{-}NOx$, $\delta^{18}O\text{-}O_3$, and temperature (equations 7-11, **Referee#1_Table 1**), γ (maximum γ and minimum γ) was estimated by Monte Carlo simulation nested in Bayesian mixing model (Zong et al., 2017). Assuming no kinetic isotope fractionation, the nitrogen isotope fractionation value in the formation process of NO_3^- (εN) was calculated by equations 11-14 combined with γ and temperature (Zong et al., 2017; Walters and Michalski, 2016; Walters et al., 2016). The εN value in our sampling period was 5.1±2.5‰, which was comparable to that in Beijing(average 6.5‰)(Fan et al., 2020). The contributions of different sources to atmospheric NOx were quantified by Bayesian mixing model coupled with εN, $\delta^{15}N$-atmospheric-NO_3^-, and $\delta^{15}N$-NOx endmembers. We have added the methods in the marked revised manuscript, **lines 169-211.**

$$\delta^{18}O\text{-}NO_3^- = \gamma \times [\delta^{18}O\text{-}NO_3^-]_{OH} + (1-\gamma) \times [\delta^{18}O\text{-}NO_3^-]_{H_2O} = \gamma \times [\delta^{18}O\text{-}HNO_3]_{OH} + (1-\gamma) \times [\delta^{18}O\text{-}HNO_3]_{H_2O} \quad (7)$$

$$[\delta^{18}O\text{-}HNO_3]_{OH} = \frac{2}{3}[(\delta^{18}O\text{-}NO_2)]_{OH} + \frac{1}{3}[\delta^{18}O\text{-}OH]_{OH} = \frac{2}{3}\left[\frac{1000\times(^{18}\alpha_{NO_2/NO}-1)(1-f_{NO_2})}{(1-f_{NO_2})+(^{18}\alpha_{NO_2/NO}\times f_{NO_2})} + [\delta^{18}O\text{-}NO_X]\right] + \frac{1}{3}[(\delta^{18}O\text{-}H_2O) + 1000\times(^{18}\alpha_{OH/H_2O}-1)] \quad (8)$$

$$[\delta^{18}O\text{-}HNO_3]_{H_2O} = \frac{5}{6}(\delta^{18}O\text{-}N_2O_5) + \frac{1}{6}(\delta^{18}O\text{-}H_2O) \quad (9)$$

$$\delta^{18}O\text{-}N_2O_5 = \delta^{18}O\text{-}NO_2 + 1000\times\left(^{18}\alpha_{N_2O_5/NO_2}-1\right) \quad (10)$$

$$1000(^{m}\alpha_{X/Y}-1) = \frac{A}{T^4}\times 10^{10} + \frac{B}{T^3}\times 10^{8} + \frac{C}{T^2}\times 10^{6} + \frac{D}{T}\times 10^{4} \quad (11)$$

$$\varepsilon N = \gamma \times \varepsilon(\delta^{15}N\text{-}NO_3^-)_{OH} + (1-\gamma)\times\varepsilon(\delta^{15}N\text{-}NO_3^-)_{H_2O} = \gamma\times\varepsilon(\delta^{15}N\text{-}HNO_3)_{OH} + (1-\gamma)\times\varepsilon(\delta^{15}N\text{-}HNO_3)_{H_2O} \quad (12)$$

$$\varepsilon(\delta^{15}N\text{-}HNO_3)_{OH} = \varepsilon(\delta^{15}N\text{-}NO_2)_{OH} = 1000\times\left[\frac{(^{15}\alpha_{NO_2/NO}-1)(1-f_{NO_2})}{(1-f_{NO_2})+(^{15}\alpha_{NO_2/NO}\times f_{NO_2})}\right] \quad (13)$$

$$\varepsilon(\delta^{15}N\text{-}HNO_3)_{H_2O} = \varepsilon(\delta^{15}N\text{-}N_2O_5)_{H_2O} = 1000\times\left(^{15}\alpha_{N_2O_5/NO_2}-1\right) \quad (14)$$

Where, γ is the contribution of ·OH formation pathway to NO_3^-, εN is the nitrogen isotope fractionation value. fNO_2 is the fraction of NO_2 in the total NOx. $^{18}\alpha NO_2/NO$, $^{18}\alpha OH/H_2O$, $^{18}\alpha N_2O_5/NO_2$ are the oxygen isotope equilibrium fractionation factors between NO_2 and NO, ·OH and H_2O, N_2O_5 and NO_2, respectively. $^{15}\alpha NO_2/NO$ and $^{15}\alpha N_2O_5/NO_2$ are the nitrogen isotope equilibrium fractionation factor between NO_2 and NO, N_2O_5 and NO_2, respectively.

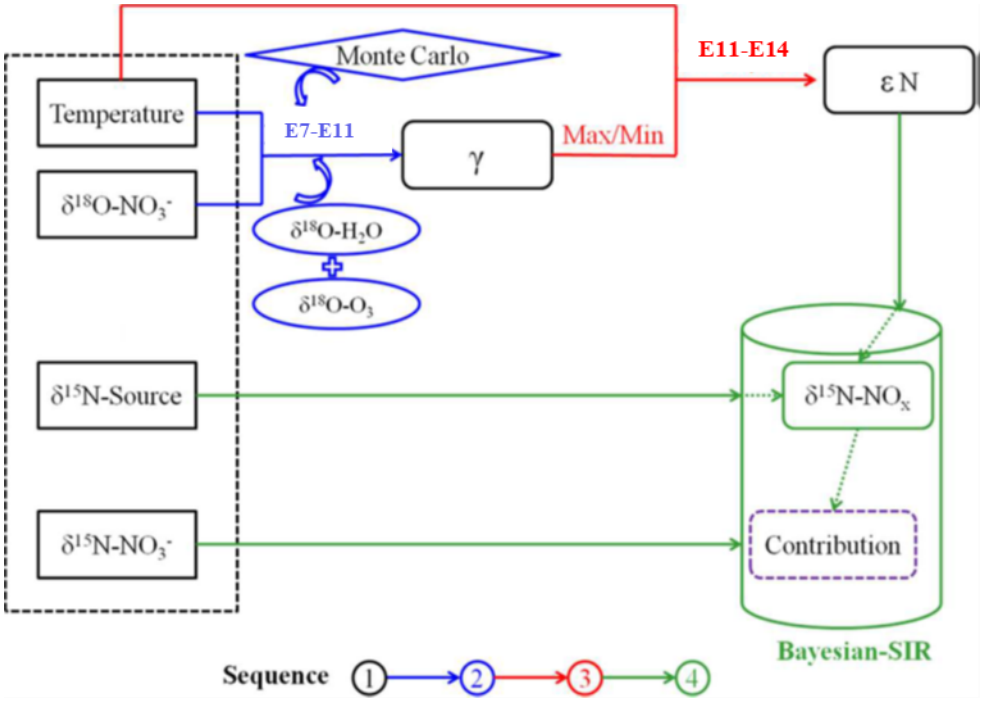

Referee#1_Figure 2. Principle and process of Bayesian mixing model in this study, the "E" represents equation in the following section, "εN" refers to N fractionation, and "SIR" is "sampling-importance-resampling"(Zong et al., 2017).

Referee#1_Table 1 (Table S1 in SI). Test constants of A, B, C, and D over the settled temperature range of 150−450K(Zong et al., 2017; Walters and Michalski, 2016; Walters and Michalski, 2015; Walters et al., 2016).

$^{m}\alpha_{X/Y}$	A	B	C	D
$^{15}NO_2/NO$	3.8834	-7.7299	6.0101	-0.17928
$^{15}N_2O_5/NO_2$	0.69398	-1.9859	2.3876	0.16308
$^{18}NO/NO_2$	-0.04129	1.1605	-1.8829	0.74723
$^{18}H_2O/OH$	2.1137	-3.8026	2.5653	0.59410

RC4: Authors should explain why these four sources are selected as main sources of atmospheric NO_3^- and these six sources are selected as main sources of atmospheric NH_4^+?

AC4： Thanks for your comment. The following was the explanation for our selection of sources of atmospheric NO_3^- and NH_4^+. We have also added the explanations in **SI Text S2.**

a. We considered coal combustion, mobile traffic sources, biomass burning, and soil microbial activity as dominant atmospheric NOx sources. Based on bottom-up emission inventory, power plant, industry, residential use, and transportation were the traditional NOx emission sources in cities in China, including Guangzhou (Liu et al., 2017). According to the type of fuel combustion, traditional sources of NOx could be roughly divided into coal combustion (power plant, industry, and residential use) and mobile sources (transportation including vehicle exhaust and ship emission). Furthermore, recent studies show that biomass burning is an essential source of NOx based on emission factor study (Mehmood et al., 2017) and isotopic evidence (Zong et al., 2020). Microbial process emission is another important source of NOx, in which nitrification or denitrification microbial bacteria widely distributed in soils consume accumulated nitrogen and release NO as a byproduct(Hall and Matson, 1996; Jaeglé et al., 2004). The cultivated land with extensive use of nitrogen fertilizer in the suburbs around Guangzhou is also an important source of NOx, which is named as microbial process in this study. δ^{15}N-NOx values differed significantly among these four sources, which allows us to differentiate their relative contributions to the mixture of atmospheric. We did not consider NO_3^- from lightning because it accounts for less than 5% of global terrestrial NOx emissions(Song et al., 2021; Qu et al., 2020; Pickering et al., 2016).

b. There are two major groups of atmospheric NH_3 emission sources(Chen et al., 2022). One is NH_3 volatilization from NH_4^+-containing substrates (mainly fertilized and natural soils, livestock, human wastes, and natural and N-polluted water). Although Guangzhou is an urban site, the emission inventory results showed a high contribution of nitrogen fertilizers application and livestock to atmospheric NH_3 (Zheng et al., 2012),

which may be influenced by agricultural activities around Guangzhou. Human waste is also an important contributor to NH_3 in cities, as suggested by a study in Shanghai(Chang et al., 2015). Guangzhou is one of China's megacities with a dense population, so the contribution of human waste to atmospheric NH_3 in Guangzhou cannot be ignored. Therefore, nitrogen fertilizers application, livestock, and human waste were considered as sources of volatilization NH_3 in this study. In addition, the other group is NH_3 associated with combustion sources (such as coal burning, vehicles, and biomass burning). The contribution of biomass burning and coal combustion to NH_3 was very high (about 76.3%) in developing countries, suggested by the global high-resolution emissions inventory (Meng et al., 2017). NH_3 in Chinese cities was indeed influenced by coal and biomass combustion evidenced by isotopes(Xiao et al., 2020; Liu et al., 2018; Pan et al., 2018). Selective catalytic reduction technology equipped with vehicles and industrial boiler is also an important source of NH_3(Meng et al., 2017). With the rapid increase in vehicle ownership, vehicle emission has a significant impact on urban NH_3, which was confirmed by tunnel tests in Guangzhou (Liu et al., 2014). Therefore, biomass burning, coal combustion, and vehicles were considered as sources of combustion NH_3 in this study.

RC5: Lines 176-178: Does the combustion of sugarcane leaf emit NH_4^+ directly or emit NH_3 and then formed NH_4^+?

AC5: We have no field measurements of smoke and particulate matter released by sugarcane burning. Gases such as NH_3, NOx, and HCN can be released during biomass burning (Zhou et al., 2006; Stubenberger et al., 2008). Therefore, we speculate that NH_3 was released directly from the burning of sugarcane leaves, and then converted into NH_4^+ by atmospheric aging. Now, we have rewritten lines 176-178. The new sentence was shown in the marked manuscript **lines 267-269:** The $\delta^{15}N$ of NH_4^+ formed from NH_3 released by sugarcane leaves burning was 44.1‰ (SI Text S3), which was consistent with the highest $\delta^{15}N$-NH_4^+ values (45.5‰ and 45.1‰) in July.

RC6: Lines 236-237: The sources apportionment results of atmospheric NO_3^- in Figure c does not correspond to that in Figure b.

AC6: We are sorry for making this mistake. Thanks for your reminding. The colors in Figure 2a and 2b do not match the previous colors in Figure 2c. Now, we have corrected this error as shown below and in the marked manuscript, **line 329**.

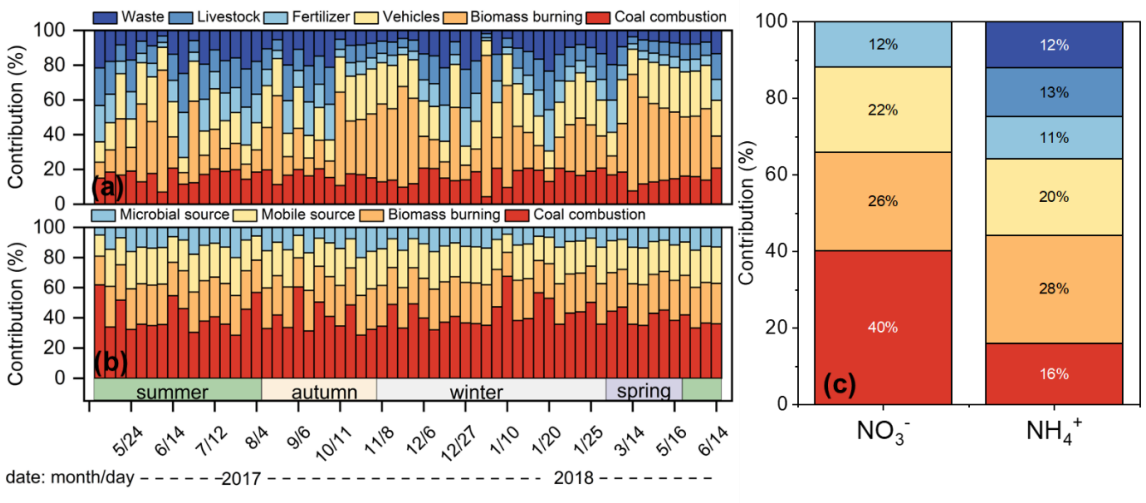

Referee#1_Figure 3 (Figure 2 in manuscript). The sources apportionment results of atmospheric NH_4^+ (a) and NO_3^- (b) in Guangzhou, and the comparison of sources results between NH_4^+ and NO_3^- (c).

RC7: Lines 272-273: Why does the author only consider the OH radical oxidation and N_2O_5 hydrolysis pathway to NO_3^-, and not consider other pathways? The author needs to explain.

AC7: Thanks for your comment and suggestion.

There are several major formation pathways of NO_3^-.

P1 (NO_2+·OH), NO_2 is oxidized by ·OH to form HNO_3, then reacts with alkaline substances (such as NH_3) to form NO_3^-.

P2 (N_2O_5), NO_2 is oxidized by O_3 to form ·NO_3, ·NO_3 reacts with NO_2 to form N_2O_5, then the hydrolysis of N_2O_5 on aerosol surfaces produces NO_3^-.

P3 (·NO_3+org), the NO_2 is oxidized by O_3 to form ·NO_3, then the ·NO_3 reacts with organic, such as dimethyl sulfide (DMS) or hydrocarbons (HC) to form HNO_3, and then NO_3^-.

P4($\cdot NO_3$+$\cdot HO_2$), NO_2 is oxidized by O_3 to form $\cdot NO_3$, $\cdot NO_3$ reacts with $\cdot HO_2$ to form HNO_3.

The P1 ($\cdot OH$) and P2 (N_2O_5) pathways are dominant formation pathways. Song reported that $\cdot OH$ and N_2O_5 pathways contributed 43% and 32% to NO_3^-, respectively, by isotope tracing (Song et al., 2021). Based on isotopic estimates, the contribution of ·NO3+org to NO_3^- was relatively high, e.g., about 16% in Beijing(Song et al., 2021). However, the proportion of $\cdot NO_3$+org estimated by the Community Multiscale Air Quality (CAMQ) model was very low in the YRD(Sun et al., 2022) and PRD(Qu et al., 2021), especially in Guangzhou (central PRD) where it is only 4%(Qu et al., 2021). The $\cdot OH$ and N_2O_5 were the dominant pathways and contributed 94% to NO_3^- in Guangzhou (Qu et al., 2021). We speculate that the different contribution of $\cdot NO_3$+org pathway between Guangzhou and Beijing may be caused by the difference in atmospheric oxidation. The ozone pollution is serious in Guangzhou due to a unique synoptic system including the surface high-pressure system, hurricane movement, and sea–land breeze(Tan et al., 2019). And the atmospheric $\cdot OH$ reactivity in Guangzhou was higher than in several cities, including Beijing (Tan et al., 2019). Take DMS as an example, the main oxidant of DMS is $\cdot OH$ (Andreae and Crutzen, 1997). However, in the cold season or remote regions, the $\cdot NO_3$ radical can also play an important role in reaction with DMS (addition reaction and hydrogen abstraction) (Andreae and Crutzen, 1997; Yin et al., 1990). The high reactivity of $\cdot OH$ may reduce the contribution of $\cdot NO_3$ to DMS in Guangzhou due to the competition between $\cdot OH$ and $\cdot NO_3$ to react with DMS. Therefore, the contribution of $\cdot NO_3$+org to NO_3^- was relatively low. In addition, the $\delta^{18}O$ of NO_3^- formed by the N_2O_5 and $\cdot NO_3$+org pathway is similar(Walters and Michalski, 2016). The introduction of the $\cdot NO_3$+org pathway would greatly increase the uncertainty of the contribution of N_2O_5 pathways. While the $\delta^{18}O$ of NO_3^- formed by the $\cdot OH$ and N_2O_5 pathway differ significantly, which allows to differentiate their relative contributions to NO_3^-. Therefore, we only considered the $\cdot OH$ and N_2O_5 pathways in this study. We have also added the explanation in **SI text S2**.

References:

Andreae, M. O. and Crutzen, P. J.: Atmospheric aerosols: biogeochemical sources and role in atmospheric chemistry, Science, 276, 1052-1058, https://doi.org/10.1126/science.276.5315.1052, 1997.

Baskaran, M., K., B. S., and F., M. D.: Oxygen isotope dynamics of atmospheric nitrate and its precursor molecules. In Handbook of Environmental Isotope Geochemistry., Springer-Verlag Berlin Heidelberg2011.

Chang, Y., Deng, C., Dore, A. J., and Zhuang, G.: Human Excreta as a Stable and Important Source of Atmospheric Ammonia in the Megacity of Shanghai, PLoS One, 10, e0144661, https://doi.org/10.1371/journal.pone.0144661, 2015.

Chen, Z. L., Song, W., Hu, C. C., Liu, X. J., Chen, G. Y., Walters, W. W., Michalski, G., Liu, C. Q., Fowler, D., and Liu, X. Y.: Significant contributions of combustion-related sources to ammonia emissions, Nat. Commun., 13, 7710, https://doi.org/10.1038/s41467-022-35381-4, 2022.

Fan, M. Y., Zhang, Y. L., Lin, Y. C., Cao, F., Zhao, Z. Y., Sun, Y., Qiu, Y., Fu, P., and Wang, Y.: Changes of emission sources to nitrate aerosols in Beijing after the clean air actions: evidence from dual isotope compositions, J. Geophys. Res.: Atmos., 125, 031998, https://doi.org/10.1029/2019jd031998, 2020.

Fang, Y. T., Koba, K., Wang, X. M., Wen, D. Z., Li, J., Takebayashi, Y., Liu, X. Y., and Yoh, M.: Anthropogenic imprints on nitrogen and oxygen isotopic composition of precipitation nitrate in a nitrogen-polluted city in southern China, Atmos. Chem. Phys., 11, 1313-1325, https://doi.org/10.5194/acp-11-1313-2011, 2011.

Hall, S. J. and Matson, P. A.: NOx emissions from soil: implications for air quality modeling in agricultural regions, Annu. Rev. Energy Environ., 21, 311-346, https://doi.org/10.1146/annurev.energy.21.1.311, 1996.

Heaton, T. H. E., Spiro, B., and Robertson, S. M. C.: Potential canopy influences on the isotopic composition of nitrogen and sulphur in atmospheric deposition, Oecologia, 109, 600-607, 1997.

Huang, S., Elliott, E. M., Felix, J. D., Pan, Y., Liu, D., Li, S., Li, Z., Zhu, F., Zhang, N., Fu, P., and Fang, Y.: Seasonal pattern of ammonium ^{15}N natural abundance in precipitation at a rural forested site and implications for NH_3 source partitioning, Environ. Pollut., 247, 541-549, https://doi.org/10.1016/j.envpol.2019.01.023, 2019.

Jaeglé, L., Martin, R. V., Chance, K., Steinberger, L., Kurosu, T. P., Jacob, D. J., Modi, A. I., Yoboué, V., Sigha-Nkamdjou, L., and Galy-Lacaux, C.: Satellite mapping of rain-induced nitric oxide emissions from soils, J. Geophys. Res.: Atmos., 109, D21310, https://doi.org/10.1029/2004jd004787, 2004.

Johnston, J. C. and Thiemens, M. H.: The isotopic composition of tropospheric ozone in three environments, J. Geophys. Res.: Atmos., 102, 25395-25404, https://doi.org/10.1029/97jd02075, 1997.

Liao, B., Wu, D., Chang, Y., Lin, Y., Wang, S., and Li, F.: Characteristics of particulate SO_4^{2-}, NO_3^-, NH_4^+, and related gaseous pollutants in Guangzhou (in Chinese), Acta Sci. Circumst., 34, 1551-1559, https://doi.org/10.13671/j.hjkxxb.2014.0218, 2014.

Liu, F., Beirle, S., Zhang, Q., van der, A. R., Zheng, B., Tong, D., and He, K.: NOx emission trends over Chinese cities estimated from OMI observations during 2005 to 2015, Atmos. Chem. Phys., 17, 9261-9275, https://doi.org/10.5194/acp-17-9261-2017, 2017.

Liu, J., Ding, P., Zong, Z., Li, J., Tian, C., Chen, W., Chang, M., Salazar, G., Shen, C., Cheng, Z., Chen, Y., Wang, X., Szidat, S., and Zhang, G.: Evidence of rural and suburban sources of urban haze formation in China: a case study from the Pearl River Delta region, J. Geophys. Res.: Atmos., 123,

4712-4726, https://doi.org/10.1029/2017jd027952, 2018.

Liu, T., Wang, X., Wang, B., Ding, X., Deng, W., Lü, S., and Zhang, Y.: Emission factor of ammonia (NH_3) from on-road vehicles in China: tunnel tests in urban Guangzhou, Environ. Res. Lett., 9, 064027, https://doi.org/10.1088/1748-9326/9/6/064027, 2014.

Mehmood, K., Chang, S., Yu, S., Wang, L., Li, P., Li, Z., Liu, W., Rosenfeld, D., and Seinfeld, J. H.: Spatial and temporal distributions of air pollutant emissions from open crop straw and biomass burnings in China from 2002 to 2016, Environ. Chem. Lett., 16, 301-309, https://doi.org/10.1007/s10311-017-0675-6, 2017.

Meng, W., Zhong, Q., Yun, X., Zhu, X., Huang, T., Shen, H., Chen, Y., Chen, H., Zhou, F., Liu, J., Wang, X., Zeng, E. Y., and Tao, S.: Improvement of a global high-resolution ammonia emission inventory for combustion and industrial sources with new data from the residential and transportation sectors, Environ. Sci. Technol., 51, 2821-2829, https://doi.org/10.1021/acs.est.6b03694, 2017.

Michalski, G., Bhattacharya, S. K., and Girsch, G.: NOx cycle and the tropospheric ozone isotope anomaly: an experimental investigation, Atmos. Chem. Phys., 14, 4935-4953, https://doi.org/10.5194/acp-14-4935-2014, 2014.

Pan, Y., Tian, S., Liu, D., Fang, Y., Zhu, X., Gao, M., Wentworth, G. R., Michalski, G., Huang, X., and Wang, Y.: Source Apportionment of Aerosol Ammonium in an Ammonia-Rich Atmosphere: An Isotopic Study of Summer Clean and Hazy Days in Urban Beijing, J. Geophys. Res.: Atmos., 123, 5681-5689, https://doi.org/10.1029/2017jd028095, 2018.

Pickering, K. E., Bucsela, E., Allen, D., Ring, A., Holzworth, R., and Krotkov, N.: Estimates of lightning NOx production based on OMI NO_2 observations over the Gulf of Mexico, J. Geophys. Res.: Atmos., 121, 8668-8691, https://doi.org/10.1002/2015jd024179, 2016.

Qu, K., Wang, X., Xiao, T., Shen, J., Lin, T., Chen, D., He, L. Y., Huang, X. F., Zeng, L., Lu, K., Ou, Y., and Zhang, Y.: Cross-regional transport of $PM_{2.5}$ nitrate in the Pearl River Delta, China: Contributions and mechanisms, Sci. Total Environ., 753, 142439, https://doi.org/10.1016/j.scitotenv.2020.142439, 2021.

Qu, Z., Henze, D. K., Cooper, O. R., and Neu, J. L.: Impacts of global NOx inversions on NO_2 and ozone simulations, Atmos. Chem. Phys., 20, 13109-13130, https://doi.org/10.5194/acp-20-13109-2020, 2020.

Song, W., Liu, X. Y., and Liu, C. Q.: New Constraints on Isotopic Effects and Major Sources of Nitrate in Atmospheric Particulates by Combining $\delta^{15}N$ and $\Delta^{17}O$ Signatures, J. Geophys. Res.: Atmos., 126, https://doi.org/10.1029/2020jd034168, 2021.

Stubenberger, G., Scharler, R., Zahirović, S., and Obernberger, I.: Experimental investigation of nitrogen species release from different solid biomass fuels as a basis for release models, Fuel, 87, 793-806, https://doi.org/10.1016/j.fuel.2007.05.034, 2008.

Sun, J., Qin, M., Xie, X., Fu, W., Qin, Y., Sheng, L., Li, L., Li, J., Sulaymon, I. D., Jiang, L., Huang, L., Yu, X., and Hu, J.: Seasonal modeling analysis of nitrate formation pathways in Yangtze River Delta region, China, Atmos. Chem. Phys., 22, 12629-12646, https://doi.org/10.5194/acp-22-12629-2022, 2022.

Tan, Z., Lu, K., Jiang, M., Su, R., Wang, H., Lou, S., Fu, Q., Zhai, C., Tan, Q., Yue, D., Chen, D., Wang, Z., Xie, S., Zeng, L., and Zhang, Y.: Daytime atmospheric oxidation capacity in four Chinese megacities during the photochemically polluted season: a case study based on box model simulation, Atmos. Chem. Phys., 19, 3493–3513, https://doi.org/10.5194/acp-19-3493-2019, 2019.

Urey, H. C.: The thermodynamic properties of isotopic substances, J. Chem. Soc., 562-581,

https://doi.org/10.1039/jr9470000562, 1947.

Walters, W. W. and Michalski, G.: Theoretical calculation of nitrogen isotope equilibrium exchange fractionation factors for various NOy molecules, Geochim. Cosmochim. Ac., 164, 284-297, https://doi.org/10.1016/j.gca.2015.05.029, 2015.

Walters, W. W. and Michalski, G.: Theoretical calculation of oxygen equilibrium isotope fractionation factors involving various NOy molecules, OH, and H_2O and its implications for isotope variations in atmospheric nitrate, Geochim. Cosmochim. Ac., 191, 89–101 https://doi.org/10.1016/j.gca.2016.06.039, 2016.

Walters, W. W., Simonini, D. S., and Michalski, G.: Nitrogen isotope exchange between NO and NO_2 and its implications for $\delta^{15}N$ variations in tropospheric NOx and atmospheric nitrate, Geophys. Res. Lett., 43, 440-448, https://doi.org/10.1002/2015gl066438, 2016.

Xiao, H. W., Wu, J. F., Luo, L., Liu, C., Xie, Y. J., and Xiao, H. Y.: Enhanced biomass burning as a source of aerosol ammonium over cities in central China in autumn, Environ. Pollut., 266, 115278, https://doi.org/10.1016/j.envpol.2020.115278, 2020.

Yin, F., Grosjean, D., and Seinfeld, J. H.: Photooxidation of Dimethyl Sulfide and Dimethyl Disulfide. I: Mechanism Development, J. Atmos. Chem., 11, 309-364, 1990.

Zheng, J. Y., Yin, S. S., Kang, D. W., Che, W. W., and Zhong, L. J.: Development and uncertainty analysis of a high-resolution NH_3 emissions inventory and its implications with precipitation over the Pearl River Delta region, China, Atmos. Chem. Phys., 12, 7041-7058, https://doi.org/10.5194/acp-12-7041-2012, 2012.

Zhou, H., Jensen, A. D., Glarborg, P., and Kavaliauskas, A.: Formation and reduction of nitric oxide in fixed-bed combustion of straw, Fuel, 85, 705-716, https://doi.org/10.1016/j.fuel.2005.08.038, 2006.

Zong, Z., Tan, Y., Wang, X., Tian, C., Li, J., Fang, Y., Chen, Y., Cui, S., and Zhang, G.: Dual-modelling-based source apportionment of NOx in five Chinese megacities: providing the isotopic footprint from 2013 to 2014, Environ. Int., 137, 105592, https://doi.org/10.1016/j.envint.2020.105592, 2020.

Zong, Z., Wang, X., Tian, C., Chen, Y., Fang, Y., Zhang, F., Li, C., Sun, J., Li, J., and Zhang, G.: First assessment of NOx sources at a regional background site in North China using isotopic analysis linked with modeling, Environ. Sci. Technol., 51, 5923-5931, https://doi.org/10.1021/acs.est.6b06316, 2017.

Response to Referee #2

RC- Reviewer's Comments; AC – Authors' Response Comments

RC1: This paper estimated the relative contributions of main sources to ammonium and nitrate aerosols in a subtropical megacity of South China using stable N isotope analysis. They found that anthropogenic activities (e.g., coal combustion, biomass burning and vehicle exhaust) are important sources and should be considered seriously in future for the improvement of air quality. In my opinion, few studies simultaneously reported 15N signatures for both NH_4^+ and NO_3^- and I think this one-year dataset is valuable and probably will improve our knowledge on the sources of air pollution. I support its publication after some minor revisions.

AC1: Thanks for your recognition of our work and for providing professional comments and valuable suggestions. These comments and suggestions are valuable and helpful for improving our manuscript. We have made revisions based on these comments (The detailed corrections are marked in the revised manuscript). If you have any further comments and suggestions, we will try our best to improve our manuscript.

RC2: Line 66-68: The dominant source of atmospheric NH_3 highly depends on the scale of study area. For example, the dominant emitter of NH_3 in the whole China should be the agricultural source; while the dominant emitter may be the vehicular emission for a city site. Therefore, cautions need to be taken when you describe this sentence.

AC2: Thanks for your professional comments. We agree with you that the dominant emitter of NH_3 in the whole China should be the agricultural source; while the dominant emitter may be the vehicular emission for a city site. In addition, there is a potential impact of biomass burning in suburban areas on urban NH_3. In general, biomass burning activity increases during autumn in Central China. Xiao et al. found that biomass burning contributed 34.5 ± 20.4%, 46.4 ± 21.4%, and 40.4 ± 17.4% to NH_4^+ for three urban sites Nanchang, Wuhan, and Changsha, respectively, during autumn(Xiao et al., 2020). The combustion sources in Lines 66-68 represent coal combustion, vehicle emission, and biomass burning. Now, we have rewritten this sentence, as shown in the

marked revised manuscript **lines 75-78**: Biomass burning in the suburbs also has a potential impact on urban NH_3(Xiao et al., 2020). As for urban NH_3, combustion sources (including coal combustion, vehicles emission, and biomass burning) were gradually becoming dominant sources in recent years verified by δ^{15}N-NHx (NH_3+NH_4^+)(Xiao et al., 2020; Pan et al., 2018).

RC3: Line 122-126: Many δ^{15}N-NH_3 endmembers of sources were collected by passive samplers. Did you correct these values when you conducted the source apportionment? Also, the endmembers and source numbers are important parameters for δ^{15}N-derived source apportionment model and I suggest you add these in the main manuscript.

AC3: Thanks for your kind suggestion. We considered and corrected the difference of δ^{15}N-NH_3 values resulting by passive samplers. The δ^{15}N-NH_3 values collected by passive samplers were significantly lower than that of the active sampler, with a difference of 15.4 ± 3.5‰(Pan et al., 2020). The δ^{15}N of NH_3 from fertilizer, livestock, and urban waste collected by passive sampler(Chang et al., 2016; Felix et al., 2013; Bhattarai et al., 2020) were corrected using 15.4 ± 3.5‰ (Bhattarai et al., 2021; Pan et al., 2020). In addition, we have added the parameters of δ^{15}N of NH_3 from different sources, as shown in **line 212** (**Table 1** in marked manuscript).

Referee#2_ Table 1 (**Table 1** in manuscript)**.** The estimation of δ^{15}N-NH_3 and δ^{15}N-NOx from various sources.

Source	δ^{15}N-NH_3(‰)	References
Biomass burning	17.5±7.8	(Kawashima and Kurahashi, 2011; Xiao et al., 2020)
Coal combustion	-2.5±6.4	(Felix et al., 2013; Pan et al., 2016)
Urban traffic	6.6±2.1	(Walters et al., 2020)
Fertilizer	-28.3±5.8	(Bhattarai et al., 2021; Chang et al., 2016; Felix et al., 2013; Bhattarai et al., 2020)
Livestock	-18.3±7.7	(Bhattarai et al., 2021; Chang et al., 2016; Felix et al., 2013; Bhattarai et al., 2020)
Urban waste	-22.8±3.6	(Bhattarai et al., 2021; Chang et al., 2016)
Source	δ^{15}N-NOx(‰)	References
Biomass burning	1.04±4.13	(Zong et al., 2017; Fibiger and Hastings, 2016; Zong et al., 2022)
Coal combustion	13.72±4.57	(Zong et al., 2017; Felix et al., 2015; Felix et al.,

		2012)
Mobile source	-7.25±7.80	(Zong et al., 2017; Walters et al., 2015)
Soil microbial process	-33.77±12.16	(Zong et al., 2017; Felix and Elliott, 2013)

RC4: Line 149: Fig 1. Can you please highlight/mark the seasonal periods in this figure? I think this will improve the readability because you mentioned the seasonal values.

AC4: Thanks for your kind suggestion. We have marked the season in **Figure 1**, as shown in the marked manuscript **line 236**.

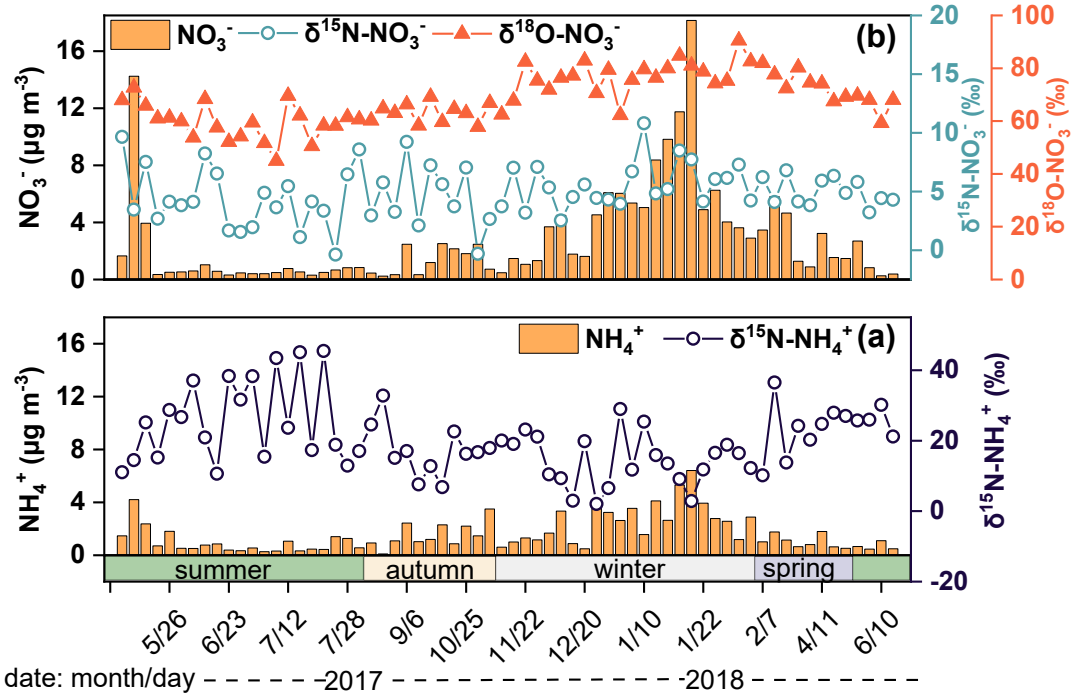

Referee#2_Figure 1(Figure 1 in manuscript). The concentration and $\delta^{15}N$ of NH_4^+ (a) and concentration, $\delta^{15}N$, and $\delta^{18}O$ of NO_3^- (b).

RC5: Line 157: "average+"?

AC5: We apologize for the confusion caused by "average+". The plus symbol ("+") means positive number. Now we have deleted the + symbol, as shown in the marked manuscript **lines 245-246**.

RC6: Line 163: It would be better to provide the way you got the NH_3 concentration in the main manuscript.

AC6: We are sorry for that we don't measure the NH_3 concentration. The proportion of the initial NH_3 converted to NH_4^+ (f, $NH_4^+/(NH_3+NH_4^+)$) for different months referenced from a previous study in Guangzhou(Liao et al., 2014).

RC7: Line 238/274 (Fig2, Fig3): again, please highlight/mark the seasonal periods (spring, summer, autumn, and winter).

AC7: Thanks for your kind suggestion. We have marked the season in Figure 2 and Figure 3, as shown in the marked manuscript **line 329** and **line 368**.

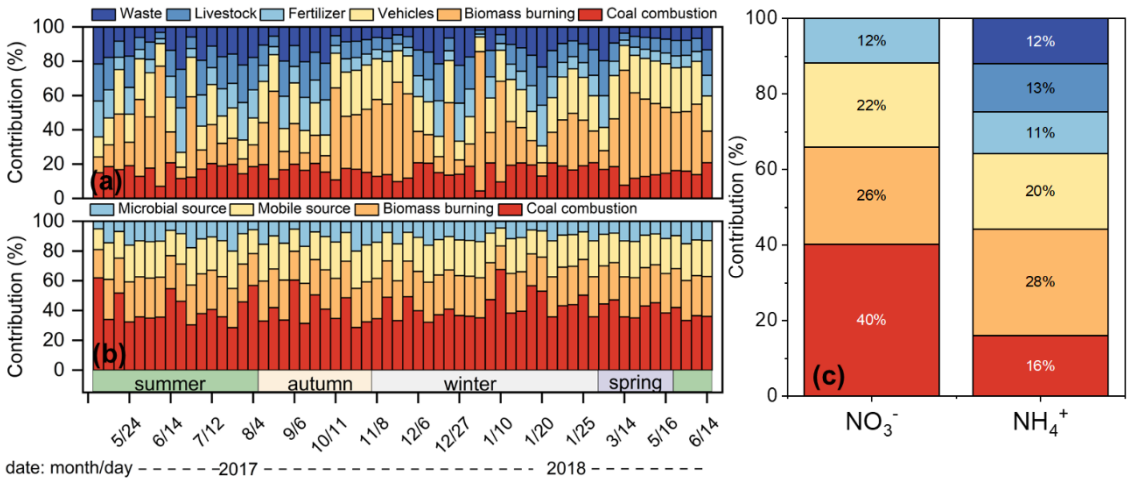

Referee#2_Figure 2 (Figure 2 in manuscript). The sources apportionment results of atmospheric NH_4^+ (a) and NO_3^- (b) in Guangzhou, and the comparison of sources results between NH_4^+ and NO_3^- (c).

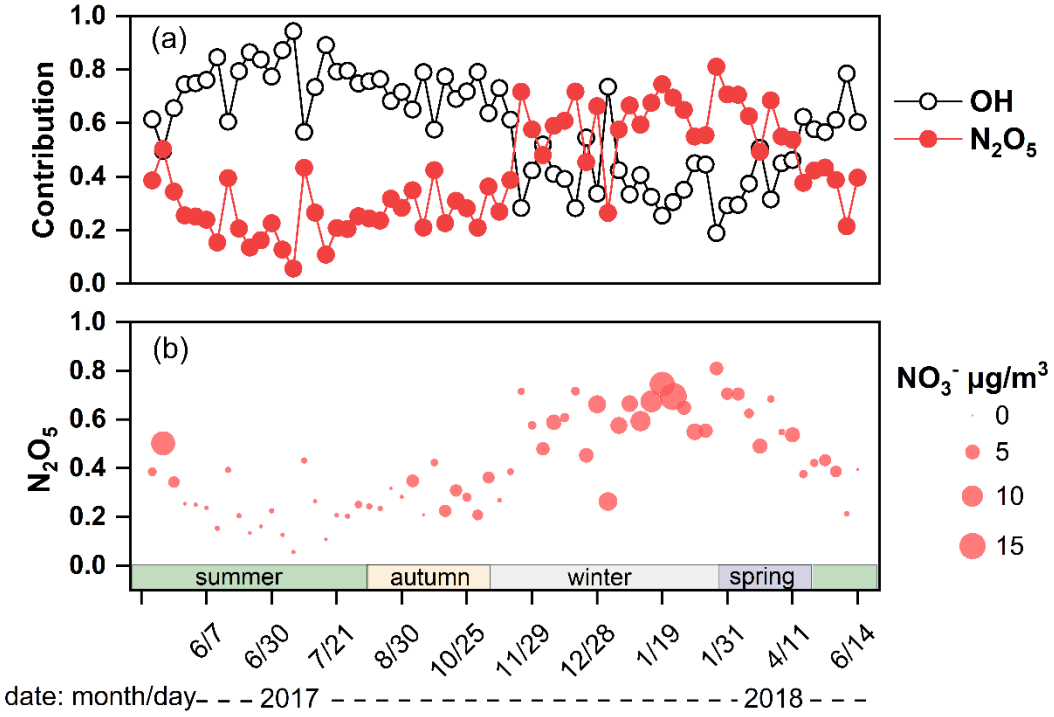

Referee#2_Figure 3 (Figure 3 in manuscript). The contribution of the OH radical oxidation and N_2O_5 hydrolysis pathway to NO_3^- (a). The vertical position of the dots corresponded to the contribution of N_2O_5 pathway and the size of the dots corresponded to the concentration of NO_3^- (b).

RC8: Line 291-292: Why you defined BeiChengHuang Island and Heshan as the sites receiving strong anthropogenic impact? These two sites are not located in cities and should be impacted less anthropogenic activities than megacities such as Beijing and Guangzhou.

AC8: Firstly, we apologize for the wrong place name "BeiChengHuang Island". It should be BeiHuangCheng Island. We have revised it in the marked manuscript. Secondly, we doubtless agree with you that these two sites are not located in cities. However, in winter, 74% of the air mass in Beihuangcheng Island come directly from the heavily polluted Beijing-Tianjin-Hebei region(Zong, 2017). And about 26% of the air mass reached Beihuangcheng Island from the Beijing-Tianjin-Hebei region through the Shandong Peninsula(Zong, 2017). Zong et al. reported that coal combustion, mobile source, and biomass burning contributed 86.3% to NO_3^- in Beihuangcheng Island, as

shown in the following figure (Zong et al., 2017). The Heshan Atmospheric Environment Monitoring Superstation is a rural station located 50 km southwest of Guangzhou (Xu et al., 2022). During the winter northeast-monsoon season, Heshan site well intercepts high anthropogenically dominated outflow airmass from Chinese continental(Xu et al., 2022). The anthropogenic sources (including fossil and biomass burning) accounted for 78% of total oxalic acid, tracers of aqueous secondary organic aerosol, in the continental outflow samples(Xu et al., 2022). Su et al. reported that coal combustion, mobile source, and biomass burning contributed 90.6% to NO_3^- in Heshan (Su et al., 2020). Therefore, NO_3^- was predominantly derived from anthropogenic sources in Beihuangcheng island and Heshan.

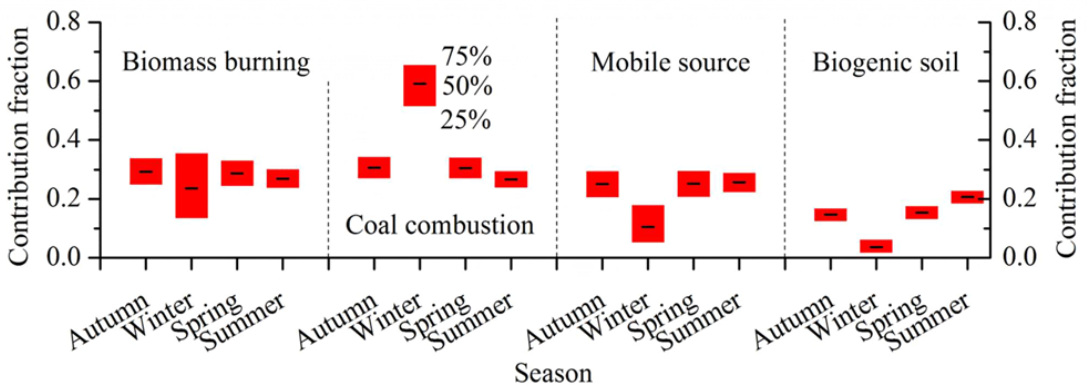

Referee#2_Figure 4. Contributions of coal combustion, mobile source, biomass burning, and biogenic soil emissions for NOx in different seasons on Beihuangcheng Island. (Zong et al., 2017)

RC9: Line 311-313. This explanation sounds reasonable. I suggest you add the references to support the facts you mentioned here (stricter vehicle emission standard, promotion of new electric vehicles etc.).

AC9: We appreciate your explicit suggestion. In order to continuously improve the Guangdong province's ambient air quality, the Guangdong Provincial Government formulated the Guangdong Air Pollution Prevention and Control Action Plan (2014-2017). The plan includes in-depth promotion of power plant pollution reduction, comprehensive promotion of boiler pollution remediation, raising the environmental

standard of new vehicles, acceleration the improvement of gasoline and diesel quality, etc(Guangdongprovince, 2014). Especially in Guangzhou and Shenzhen, clean energy vehicles will account for more than 60% of annual new buses from 2014 (Guangdongprovince, 2014). In addition, China introduced an ultra-low emissions (ULE) standards policy for renovating coal-fired power-generating units in 2014. Tang et al., found that between 2014 and 2017 China's annual power emissions of NOx dropped by 60% since the implementation of ULE policy (Tang et al., 2019). Now, we have added the above references to the marked manuscript **line 408**.

RC10: Line 324-325: "The contribution of biomass burning and vehicle was stable through a year." The vehicular emission, in my opinion, is likely constant because people drive cars in all seasons. However, the biomass burning activity generally is highly related with seasons. Can you make some explanations on this?

AC10: Thanks for your insightful comment and kind suggestion. We totally agree with you that biomass burning is highly related to the seasons. Generally, high intensity biomass burning occurred in winter in Guangdong province (dry season, i.e., from November to March)(Xu et al., 2019). K^+ is a typical tracer of biomass burning. The concentration of K^+ enhanced in winter (0.4μg/m^3) was higher than that in summer(0.2μg/m^3) and autumn(0.2μg/m^3), respectively, indicating enhancement of biomass burning intensity. Also, NO_3^- concentration of biomass burning remarkably enhanced in winter (1.2μg/m^3) and was higher than that in summer (0.4μg/m^3) and autumn (0.3μg/m^3), respectively. However, coal combustion also enhanced in winter due to the demand for heating in North China. Our sampling site was influenced by the air mass with high coal combustion contribution from the North by long-range transportation, which may reduce the contribution of biomass burning relatively. Thus, the contribution of biomass burning showed stable compared with coal combustion. We have added the explanation in the marked manuscript, **lines 421-431**.

References:

Bhattarai, N., Wang, S., Pan, Y., Xu, Q., Zhang, Y., Chang, Y., and Fang, Y.: δ^{15}N-stable isotope analysis of NHx : An overview on analytical measurements, source sampling and its source apportionment, Front. Environ. Sci. Eng., 15, 126, https://doi.org/10.1007/s11783-021-1414-6, 2021.

Bhattarai, N., Wang, S., Xu, Q., Dong, Z., Chang, X., Jiang, Y., and Zheng, H.: Sources of gaseous NH_3 in urban Beijing from parallel sampling of NH_3 and NH_4^+, their nitrogen isotope measurement and modeling, Sci. Total Environ., 747, 141361, https://doi.org/10.1016/j.scitotenv.2020.141361, 2020.

Chang, Y., Liu, X., Deng, C., Dore, A. J., and Zhuang, G.: Source apportionment of atmospheric ammonia before, during, and after the 2014 APEC summit in Beijing using stable nitrogen isotope signatures, Atmos. Chem. Phys., 16, 11635-11647, https://doi.org/10.5194/acp-16-11635-2016, 2016.

Felix, J. D. and Elliott, E. M.: The agricultural history of human-nitrogen interactions as recorded in ice core δ^{15}N-NO_3^-, Geophys. Res. Lett., 40, 1642-1646, https://doi.org/10.1002/grl.50209, 2013.

Felix, J. D., Elliott, E. M., and Shaw, S. L.: Nitrogen isotopic composition of coal-fired power plant NOx: influence of emission controls and implications for global emission inventories, Environ. Sci. Technol., 46, 3528-3535, https://doi.org/10.1021/es203355v, 2012.

Felix, J. D., Elliott, E. M., Gish, T. J., McConnell, L. L., and Shaw, S. L.: Characterizing the isotopic composition of atmospheric ammonia emission sources using passive samplers and a combined oxidation-bacterial denitrifier approach, Rapid Commun. Mass Spectrom., 27, 2239-2246, https://doi.org/10.1002/rcm.6679, 2013.

Felix, J. D., Elliott, E. M., Avery, G. B., Kieber, R. J., Mead, R. N., Willey, J. D., and Mullaugh, K. M.: Isotopic composition of nitrate in sequential Hurricane Irene precipitation samples: Implications for changing NOx sources, Atmos. Environ., 106, 191-195, https://doi.org/10.1016/j.atmosenv.2015.01.075, 2015.

Fibiger, D. L. and Hastings, M. G.: First Measurements of the Nitrogen Isotopic Composition of NOx from Biomass Burning, Environ. Sci. Technol., 50, 11569-11574, https://doi.org/10.1021/acs.est.6b03510, 2016.

Action Plan for Air Pollution Control of Guangdong Province (2014-2017): http://www.gd.gov.cn/gkmlpt/content/0/142/mpost_142687.html, last access: February 14, 2014.

Kawashima, H. and Kurahashi, T.: Inorganic ion and nitrogen isotopic compositions of atmospheric aerosols at Yurihonjo, Japan: implications for nitrogen sources, Atmos. Environ., 45, 6309-6316, https://doi.org/10.1016/j.atmosenv.2011.08.057, 2011.

Liao, B., Wu, D., Chang, Y., Lin, Y., Wang, S., and Li, F.: Characteristics of particulate SO_4^{2-}, NO_3^-, NH_4^+, and related gaseous pollutants in Guangzhou (in Chinese), Acta Sci. Circumst., 34, 1551-1559, https://doi.org/10.13671/j.hjkxxb.2014.0218, 2014.

Pan, Y., Tian, S., Liu, D., Fang, Y., Zhu, X., Zhang, Q., Zheng, B., Michalski, G., and Wang, Y.: Fossil fuel combustion-related emissions dominate atmospheric ammonia sources during severe haze episodes: evidence from ^{15}N-stable isotope in size-resolved aerosol ammonium, Environ. Sci. Technol., 50, 8049-8056, https://doi.org/10.1021/acs.est.6b00634, 2016.

Pan, Y., Tian, S., Liu, D., Fang, Y., Zhu, X., Gao, M., Wentworth, G. R., Michalski, G., Huang, X., and Wang, Y.: Source Apportionment of Aerosol Ammonium in an Ammonia-Rich Atmosphere: An Isotopic Study of Summer Clean and Hazy Days in Urban Beijing, J. Geophys. Res.: Atmos., 123, 5681-5689, https://doi.org/10.1029/2017jd028095, 2018.

Pan, Y., Gu, M., Song, L., Tian, S., Wu, D., Walters, W. W., Yu, X., Lü, X., Ni, X., Wang, Y., Cao, J., Liu, X., Fang, Y., and Wang, Y.: Systematic low bias of passive samplers in characterizing nitrogen

isotopic composition of atmospheric ammonia, Atmos. Res., 243, https://doi.org/10.1016/j.atmosres.2020.105018, 2020.

Su, T., Li, J., Tian, C., Zong, Z., Chen, D., and Zhang, G.: Source and formation of fine particulate nitrate in South China: Constrained by isotopic modeling and online trace gas analysis, Atmos. Environ., 231, https://doi.org/10.1016/j.atmosenv.2020.117563, 2020.

Tang, L., Qu, J., Mi, Z., Bo, X., Chang, X., Anadon, L. D., Wang, S., Xue, X., Li, S., Wang, X., and Zhao, X.: Substantial emission reductions from Chinese power plants after the introduction of ultra-low emissions standards, Nat. Energy, 4, 929-938, https://doi.org/10.1038/s41560-019-0468-1, 2019.

Walters, W. W., Tharp, B. D., Fang, H., Kozak, B. J., and Michalski, G.: Nitrogen Isotope Composition of Thermally Produced NOx from Various Fossil-Fuel Combustion Sources, Environ. Sci. Technol., 49, 11363-11371, https://doi.org/10.1021/acs.est.5b02769, 2015.

Walters, W. W., Song, L., Chai, J., Fang, Y., Colombi, N., and Hastings, M. G.: Characterizing the spatiotemporal nitrogen stable isotopic composition of ammonia in vehicle plumes, Atmos. Chem. Phys., 20, 11551-11567, https://doi.org/10.5194/acp-20-11551-2020, 2020.

Xiao, H. W., Wu, J. F., Luo, L., Liu, C., Xie, Y. J., and Xiao, H. Y.: Enhanced biomass burning as a source of aerosol ammonium over cities in central China in autumn, Environ. Pollut., 266, 115278, https://doi.org/10.1016/j.envpol.2020.115278, 2020.

Xu, B., Zhang, G., Gustafsson, O., Kawamura, K., Li, J., Andersson, A., Bikkina, S., Kunwar, B., Pokhrel, A., Zhong, G., Zhao, S., Li, J., Huang, C., Cheng, Z., Zhu, S., Peng, P., and Sheng, G.: Large contribution of fossil-derived components to aqueous secondary organic aerosols in China, Nat. Commun., 13, 5115, https://doi.org/10.1038/s41467-022-32863-3, 2022.

Xu, Y., Huang, Z., Jia, G., Fan, M., Cheng, L., Chen, L., Shao, M., and Zheng, J.: Regional discrepancies in spatiotemporal variations and driving forces of open crop residue burning emissions in China, Sci. Total Environ., 671, 536-547, https://doi.org/10.1016/j.scitotenv.2019.03.199, 2019.

Zong, Z.: Composition and source apportionment of $PM_{2.5}$ at the background area in North China, Doctor, Yantai Institute of Coastal Zone Research, Chinese Academy of Sciences, 2017.

Zong, Z., Shi, X., Sun, Z., Tian, C., Li, J., Fang, Y., Gao, H., and Zhang, G.: Nitrogen isotopic composition of NOx from residential biomass burning and coal combustion in North China, Environ. Pollut., 304, 119238, https://doi.org/10.1016/j.envpol.2022.119238, 2022.

Zong, Z., Wang, X., Tian, C., Chen, Y., Fang, Y., Zhang, F., Li, C., Sun, J., Li, J., and Zhang, G.: First assessment of NOx sources at a regional background site in North China using isotopic analysis linked with modeling, Environ. Sci. Technol., 51, 5923-5931, https://doi.org/10.1021/acs.est.6b06316, 2017.

High contribution of anthropogenic combustion sources to atmospheric inorganic reactive nitrogen in South China evidenced by isotopes

Tingting Li[1,2,4], Jun Li[*1,2], Zeyu Sun[3,4], Hongxing Jiang[1], Chongguo Tian[3], Gan Zhang[1,2]

[1]State Key Laboratory of Organic Geochemistry and Guangdong province Key Laboratory of Environmental Protection and Resources Utilization, Guangdong-Hong Kong-Macao Joint Laboratory for Environmental Pollution and Control, Guangzhou Institute of Geochemistry, Chinese Academy of Sciences, Guangzhou, 510640, China

[2]CAS Center for Excellence in Deep Earth Science, Guangzhou 510640, P. R. China

[3]Yantai Institute of Coastal Zone Research, Chinese Academy of Sciences, Yantai 264003, P. R. China

[4]University of Chinese Academy of Sciences, Beijing 100049, P. R. China

**Correspondence to*: Jun Li (junli@gig.ac.cn)

Abstract: Due to the intense release of reactive nitrogen (Nr) from anthropogenic activity, the source layout of atmospheric nitrogen aerosol has changed. The inorganic nitrogen (NH_4^+ and NO_3^-) was essential part of atmospheric nitrogen aerosol and accounted for 69%. To comprehensively clarify the level, sources, and environmental fate of NH_4^+ and NO_3^-, their concentrations and stable isotopes ($\delta^{15}N$) in fine particulate matters ($PM_{2.5}$) were measured in a subtropical megacity of South China. N-NH_4^+ and N-NO_3^- contributed 45.8% and 23.2% to total nitrogen (TN), respectively. The source contributions of NH_4^+ and NO_3^- were estimated by $\delta^{15}N$, which suggested that anthropogenic combustion activities including coal combustion, biomass burning, and vehicles were dominant sources. Especially, biomass burning was the predominant source of NH_4^+ (27.9%). Whereas, coal combustion was the dominant source of NO_3^- (40.4%). This study emphasized the substantial impacts of human activities on inorganic Nr. With the rapid development of industry and transportation, nitrogen emissions will be even higher. The promotion of clean energy and efficient use of biomass would help reduce nitrogen emissions and alleviate air pollution.

1. Introduction

Nitrogenous aerosols are ubiquitous in environment and play an important role as nutrients in ecosystems(Bhattarai et al., 2019). With the massive combustion of fossil fuels and the development of livestock, the proportion of TN in particulate matter (PM) ranges from 1.2% to 17.0% and has shown a rapid increase in the last few decades(Bhattarai et al., 2019; Galloway et al., 2004; Holland et al., 1999). Mostly nitrogenous aerosols formed from atmospheric Nr will be deposited into terrestrial and aquatic ecosystems(Huang et al., 2015). Excessive external nitrogen deposition accelerates nitrogen loss in soil, decreases species diversity, disturbs terrestrial ecosystems, and leads to eutrophication in aquatic ecosystems(Breemen, 2002; Wedin and Tilman, 1996; Yang et al., 2015). Furthermore, nitrogenous aerosols have adverse impacts on the climate, air quality, and human health(Bhattarai et al., 2019; Song et al., 2021).

N-NO_3^- and N-NH_4^+ as inorganic Nr are dominant species in the deposition of nitrogen(Zhu et al., 2015). N-NH_4^+ was the highest in nitrogen deposition, and NH_4^+ was gradually considered to be an important component of secondary inorganic aerosols (SIA)(Sun et al., 2021). NH_3, the precursor of NH_4^+, is a vital atmospheric alkaline gas, which can participate in nucleation to promote ~~the~~ new particles generation, and can react with acid gas to produce ammonium sulfate and ammonium nitrate(Dunne et al., 2016; Fu et al., 2017). The excessive NH_3 emission from anthropogenic sources will partially offset the benefits of reducing SO_2 and NOx and trigger urban haze in China(Sun et al., 2021; Meng et al., 2018; Pan et al., 2018a). In many urban environments, NO_3^- has replaced sulfate as the component with the highest proportion in SIA. NOx, precursors of NO_3^-, are also closely related to the formation of atmospheric oxidants and exert important effects on atmospheric oxidation. In addition, NH_4NO_3 in PM plays an increasingly important role in promoting the formation of sulfate and organic matter, and has profound effect on the physical and chemical properties of PM(Liu et al., 2021; Liu et al., 2020; Hodas et al., 2014). Therefore, to mitigate ~~the~~ nitrogen deposition and air pollution, the control of NH_4^+ (NH_3) and NO_3^- (NOx) should not be neglected.

Considerable efforts have been made to comprehensively understand the budget of atmospheric NH_4^+ and NO_3^-. $\delta^{15}N$ is effective to quantify sources contribution of nitrogenous

species(Elliott et al., 2007). The anthropogenic combustion sources (combustion of coal, biomass, and gasoline) play a key role in the emission of NO_3^- (NOx) in many regions of China suggested by $\delta^{15}N$(Zong et al., 2020), which also have large effects on NH_3(Chen et al., 2022b). NH_3 is released by agricultural sources (agricultural activity and livestock) and non-agricultural sources (fossil fuel combustion and vehicle)(Bhattarai et al., 2019). ~~Previous~~ A previous study showed that agricultural source was the dominant source (80%-90%) of NH_3 in China(Kang et al., 2016). However, NH_3 emissions from agricultural source have been reduced due to intensive farming and efficient fertilization(Wang et al., 2022). ~~Combustion sources were gradually becoming dominant sources of urban NH_3 in recent years verified by the methods of emission inventory and $\delta^{15}N$(Xiao et al., 2020; Meng et al., 2017). Especially, the incomplete burning of biomass leads to massive NH_3 emission and is gradually to be the second largest non-agricultural source of NH_3(Yu et al., 2020), which may be responsible for the lag of the decline in air pollutants deposition behind the reduction in emission of precursors(Zhao et al., 2022b).~~ The incomplete burning of biomass leads to massive NH_3 emissions and is gradually to be the second largest non-agricultural source of NH_3(Yu et al., 2020), which may be responsible for the lag of the decline in air pollutants deposition behind the reduction in emission of precursors(Zhao et al., 2022b). Biomass burning in the suburbs also has a potential impact on urban NH_3(Xiao et al., 2020). As for urban NH_3, combustion sources (including coal combustion, vehicles emission, and biomass burning) were gradually becoming dominant sources in recent years verified by $\delta^{15}N$-NHx (NH_3+NH_4^+)(Xiao et al., 2020; Pan et al., 2018b). In addition, the super clean emission of coal-fired power plant and strict emission standards of vehicles will change the source layout of NH_4^+ and NO_3^-. Selective catalytic reduction technology equipped with vehicles and industrial boiler reduces NOx but increases NH_3 emissions(Meng et al., 2017; Pan et al., 2016). The occurrence of haze in North China was closely related to NH_3 emissions from combustion sources(Pan et al., 2018a; Pan et al., 2018b). NH_4^+ and NO_3^- are the main components of SIA and play a vital role in the formation of secondary aerosol(Meng et al., 2017), so it is necessary to revisit their sources.

Nr emissions from densely populated subtropical areas increased rapidly with the high~~ly~~ development of industry and transportation(Wang et al., 2013). Guangzhou is the core megacity in the South subtropical region of China, where the atmospheric environment is complex and

the atmospheric oxidation level is high(Tan et al., 2019). The high emissions of inorganic nitrogen ~~form~~ from anthropogenic combustion sources have serious and profound impacts on the environment. In this study, we aimed to comprehensively clarify the level of inorganic Nr and revisit the source layout of atmospheric inorganic Nr.

2. Experimental and theoretical methods

2.1. Sampling and Chemical concentration analysis

$PM_{2.5}$ samples (n=66) were collected from May 2017 to June 2018 in Guangzhou (23.13°N, 113.27°E). Details of sample collection can be found in our previous study(Jiang et al., 2021a). The chemical components including water-soluble ions (i.e., NH_4^+, K^+, Na^+, Ca^{2+}, Mg^{2+}, Cl^-, NO_3^-, and SO_4^{2-}), organic carbon (OC), element carbon (EC), and organic molecular markers (e.g., levoglucosan) were analyzed in our previous studies (**SI Text S1**)(Jiang et al., 2021a; Jiang et al., 2021b). Moreover, meteorological parameters (temperature, relative humidity (RH), atmosphere pressure, and wind speed) and the concentration of trace gases (CO, SO_2, NO, NO_2, and O_3) were acquired by online instruments (details shown in **SI Text S1**). A circular punch (r=1cm) of the sample filter was wrapped in a tin boat and then measured in an elemental analyzer to determine the concentrations of TN.

2.2. Isotope analysis

The $\delta^{15}N\text{-}NO_3^-$ and $\delta^{18}O\text{-}NO_3^-$ values in $PM_{2.5}$ ~~was~~ were analyzed by methods of nitrous oxide (N_2O), which was described in previous study in detail(Zong et al., 2017). Briefly, NO_3^- was reduced to NO_2^- using cadmium powder and imidazole solution, and N_2O was made by adding NaN_3 to NO_2^- solution. The production of 75nmol N_2O gas was needed to measure. The N_2O gas produced by above processes was measured by MAT253 stable isotope mass spectrometer. The values of $\delta^{18}O$ and $\delta^{15}N$ were expressed in per mil (‰) shown in Eq. (1) and (2), relative to the international oxygen and nitrogen isotope standard, respectively.

$$\delta^{15}N = \left[\frac{(^{15}N/^{14}N)_{sample}}{(^{15}N/^{14}N)_{standard}} - 1\right] * 1000 \quad (1)$$

$$\delta^{18}O = \left[\frac{(^{18}O/^{16}O)_{sample}}{(^{18}O/^{16}O)_{standard}} - 1\right] * 1000 \quad (2)$$

The $\delta^{15}N\text{-}NH_4^+$ was measured by methods of hypobromite oxidation coupled with

reduction of hydroxylamine hydrochloride(Sun et al., 2021). Briefly, NH_4^+ was oxidated to NO_2^- using alkaline hypobromite (BrO^-), and N_2O was made by adding sodium arsenite and hydrochloric acid to NO_2^- solution. The production of 120 nmol N_2O gas was needed to measure. The N_2O gas produced by above processes was measured by MAT253 stable isotope mass spectrometer. The values of $\delta^{15}N$ were expressed in per mil (‰), Eq. (1). To ensure the stability of the instrument, standard samples were tested for every ten samples. The standard deviation of replicates was generally less than 0.4‰, 0.8‰, and 0.5‰ for $\delta^{15}N$-NO_3^-, $\delta^{18}O$-NO_3^-, and $\delta^{15}N$-NH_4^+, respectively. The instrumental values of $\delta^{15}N$-NO_3^- and $\delta^{18}O$-NO_3^- were corrected by multi-point correction ($\delta^{18}O$ r^2=0.99, $\delta^{15}N$ r^2=0.999) based on international standards (IAEA-NO-3, USGS32, USGS34, and USGS35). The measured values of $\delta^{15}N$-NH_4^+ were also corrected by multi-point correction (r^2=0.999) based on international standards (IAEA-N1, USGS25, and USGS26). In addition, ^7Be and ^{210}Pb were acquired and details were shown in **SI Text S1**.

2.3. IsoSource and Bayesian mixing ~~and IsoSource~~ model

IsoSource model. IsoSource model was released by Environmental Protection Agency (EPA), could calculate ranges of source contributions to a mixture based on conservation of isotopic mass when number of sources is too large to permit a unique solution and provide the distribution of source proportions (Phillips et al., 2005). IsoSource model coupled with $\delta^{15}N$-NH_3 of atmospheric initial and potential sources (shown in Table 1) were applied to quantify the contribution of various sources to NH_3. Nitrogen fertilizers application, livestock, human waste, biomass burning, coal combustion, and vehicles were considered as sources of NH_3 in this study, details shown in **SI Text S2**. Atmospheric initial $\delta^{15}N$-NH_3 was calculated by following Eq. (3).

$$\delta^{15}N\text{-}NH_{3\text{-initial}} = \delta^{15}N\text{-}NH_4^+ - \varepsilon(NH_4^+\text{-}NH_3) \times (1 - f) \quad (3)$$

Where, $\delta^{15}N$-NH_4^+ and $\delta^{15}N$-$NH_{3\text{-initial}}$ represent the $\delta^{15}N$ of particulate NH_4^+ and atmospheric initial NH_3, respectively. $\varepsilon(NH_4^+\text{-}NH_3)$ represents the isotope fractionation factor in the gaseous NH_3 conversion to particulate NH_4^+ in the atmosphere. The f value represents the proportion of the initial NH_3 converted to NH_4^+, referring to NH_3 and NH_4^+ observed in Guangzhou (Liao et al., 2014).

The $\varepsilon(NH_4^+\text{-}NH_3)$ value is temperature dependent(Huang et al., 2019), which can be deduced from(Urey, 1947), as shown in Eq. (4). The atmospheric average temperature was 24.5°C in our sampling period, and the corresponding $\varepsilon(NH_4^+\text{-}NH_3)$ value was 34.2‰ calculated by Eq. (4). In addition, the $\varepsilon(NH_4^+\text{-}NH_3)$ in Guangzhou was estimated to be 32.4‰ according to Eq. (8). Eq. (8) was deduced by Eq. (5-7). According to Eq. (8), a linear fitting equation was observed between fNH_4^+ and $\delta^{15}N\text{-}NH_4^+$ (Fig. S1), and the absolute value of the slope (32.4‰) was equal to $\varepsilon(NH_4^+\text{-}NH_3)$. The $\varepsilon(NH_4^+\text{-}NH_3)$ average of the two methods (34.2‰ and 32.4‰) was 33.3‰ and approximated to the experimental isotope enrichment factor (33‰)(Heaton et al., 1997). Therefore, 33‰ was used for deducing the $\delta^{15}N$ of the initial NH_3.

$$\varepsilon_{(NH_4^+\_NH_3)} = 12.4678 * \frac{1000}{T+273.15} - 7.6694 \quad (4)$$

$$\delta^{15}N\text{-}NH_4^+ - \delta^{15}N\text{-}NH_3 = \varepsilon_{(NH_4^+\_NH_3)} \quad (5)$$

$$fNH_4^+ + fNH_3 = 1 \quad (6)$$

$$\delta^{15}N\text{-}NH_4^+ * fNH_4^+ + \left(\delta^{15}N\text{-}NH_4^+ - \varepsilon_{(NH_4^+\_NH_3)}\right) * (1 - fNH_4^+) = \delta^{15}N \quad (7)$$

$$\delta^{15}N\text{-}NH_4^+ = -\varepsilon_{(NH_4^+\_NH_3)} * fNH_4^+ + (\delta^{15}N + \varepsilon_{(NH_4^+\_NH_3)}) \quad (8)$$

Where, T represents the atmospheric temperature (°C). $\delta^{15}N\text{-}NH_4^+$ and $\delta^{15}N\text{-}NH_3$ represent the $\delta^{15}N$ of particulate NH_4^+ and atmospheric NH_3, respectively. $\delta^{15}N$ represents the sum of $\delta^{15}N\text{-}NH_4^+$ and $\delta^{15}N\text{-}NH_3$. fNH_3 and fNH_4^+ represent the proportion of atmospheric NH_3 and particulate NH_4^+, respectively.

Bayesian mixing model. $\delta^{15}N$ were used for tracing source based on conservation of isotopic mass. Bayesian mixing model improved upon linear mixing models by explicitly considering uncertainty in prior information and isotopic equilibrium fractionation. Recently, Bayesian mixing model was applied to trace the sources of atmospheric pollutants(Zong et al., 2017; Zong et al., 2020). The model coupled with $\delta^{15}N\text{-}NO_3^-$ and $\delta^{18}O\text{-}NO_3^-$ were used to identify the formation process and quantify the sources contribution of NO_3^-.

In Central Pearl River Delta (PRD), NO_3^- formed through ·OH and N_2O_5 pathways contributed to 94% simulated by CAMQ model (Qu et al., 2021). In this study, only ·OH and N_2O_5 formation pathways were considered. Details of NO_3^- formation pathway were also shown in **SI Text S2**. The atmospheric $\delta^{18}O\text{-}NO_3^-$ can be expressed by Eq. (9). The [$\delta^{18}O$-

$HNO_3]_{OH}$ can be further expressed by Eq. (10) assuming no kinetic isotope fractionation (Walters and Michalski, 2016). And $[\delta^{18}O\text{-}HNO_3]_{H2O}$ can be estimated by Eq. (11) (Walters and Michalski, 2016). The $\delta^{18}O$ values in tropospheric H_2O, NOx, O_3, and OH were within a certain range. The tropospheric $\delta^{18}O\text{-}H_2O$, $\delta^{18}O$-NOx, $\delta^{18}O\text{-}O_3$, and $\delta^{18}O$-OH ranged from -25‰ to 0‰(Baskaran et al., 2011; Walters and Michalski, 2016), 112‰ to 122‰ (Michalski et al., 2014; Walters and Michalski, 2016), 90‰ to 122‰, and -15‰ to 0‰, respectively(Fang et al., 2011; Johnston and Thiemens, 1997). Therefore, the γ (the contribution of ·OH formation pathway) can be estimated by fNO_2 and oxygen isotope fractionation i.e., $\alpha NO_2/NO$, $\alpha OH/H_2O$, and $\alpha N_2O_5/NO_2$. The oxygen isotope fractionations are temperature dependent and can be estimated by Eq. (13) and **Table S1.** The fNO_2 varied from 0.20 to 0.95(Zong et al., 2017; Walters et al., 2016). Based on $\delta^{18}O\text{-}NO_3^-$, $\delta^{18}O\text{-}H_2O$, $\delta^{18}O$-NOx, $\delta^{18}O\text{-}O_3$, and temperature (Eq. (9-13)), γ (maximum γ and minimum γ) was estimated by Monte Carlo simulation nested in Bayesian mixing model (Zong et al., 2017). Assuming no kinetic isotope fractionation, the nitrogen isotope fractionation value in the formation process of NO_3^- (εN) was calculated by Eq. (13-16) combined with γ and temperature (Zong et al., 2017; Walters and Michalski, 2016; Walters et al., 2016). The εN value in our sampling period was 5.1±2.5‰, which was comparable to that in Beijing(average 6.5‰)(Fan et al., 2020). The contributions of different sources to atmospheric NOx were quantified by Bayesian mixing model coupled with εN, $\delta^{15}N$-atmospheric-NO_3^-, and $\delta^{15}N$-NOx endmembers shown in **Table 1**. We considered coal combustion, mobile traffic sources, biomass burning, and soil microbial process as dominant atmospheric NOx sources in Guangzhou, details shown in **SI Text S2**. The specific details of Bayesian mixing model were reported by our previous studies(Zong et al., 2017; Zong et al., 2020).

$$\delta^{18}O\text{-}NO_3^- = \gamma \times [\delta^{18}O\text{-}NO_3^-]_{OH} + (1-\gamma) \times [\delta^{18}O\text{-}NO_3^-]_{H_2O} = \gamma \times [\delta^{18}O\text{-}HNO_3]_{OH} + (1-\gamma) \times [\delta^{18}O\text{-}HNO_3]_{H_2O} \quad (9)$$

$$[\delta^{18}O\text{-}HNO_3]_{OH} = \frac{2}{3}[(\delta^{18}O\text{-}NO_2)]_{OH} + \frac{1}{3}[\delta^{18}O\text{-}OH]_{OH} = \frac{2}{3}\left[\frac{1000\times(^{18}\alpha_{NO_2/NO}-1)(1-f_{NO_2})}{(1-f_{NO_2})+(^{18}\alpha_{NO_2/NO}\times f_{NO_2})} + [\delta^{18}O\text{-}NO_X]\right] + \frac{1}{3}[(\delta^{18}O\text{-}H_2O) + 1000\times(^{18}\alpha_{OH/H_2O}-1)] \quad (10)$$

$$[\delta^{18}O\text{-}HNO_3]_{H_2O} = \frac{5}{6}(\delta^{18}O\text{-}N_2O_5) + \frac{1}{6}(\delta^{18}O\text{-}H_2O) \quad (11)$$

$$\delta^{18}O\text{-}N_2O_5 = \delta^{18}O\text{-}NO_2 + 1000 \times \left({}^{18}\alpha_{N_2O_5/NO_2} - 1\right) \quad (12)$$

$$1000({}^{m}\alpha_{X/Y} - 1) = \frac{A}{T^4} \times 10^{10} + \frac{B}{T^3} \times 10^{8} + \frac{C}{T^2} \times 10^{6} + \frac{D}{T} \times 10^{4} \quad (13)$$

$$\varepsilon N = \gamma \times \varepsilon(\delta^{15}N\text{-}NO_3^-)_{OH} + (1-\gamma) \times \varepsilon(\delta^{15}N\text{-}NO_3^-)_{H_2O}$$
$$= \gamma \times \varepsilon(\delta^{15}N\text{-}HNO_3)_{OH} + (1-\gamma) \times \varepsilon(\delta^{15}N\text{-}HNO_3)_{H_2O} \quad (14)$$

$$\varepsilon(\delta^{15}N\text{-}HNO_3)_{OH} = \varepsilon(\delta^{15}N\text{-}NO_2)_{OH} = 1000 \times \left[\frac{({}^{15}\alpha_{NO_2/NO}-1)(1-f_{NO_2})}{(1-f_{NO_2})+({}^{15}\alpha_{NO_2/NO} \times f_{NO_2})}\right] \quad (15)$$

$$\varepsilon(\delta^{15}N\text{-}HNO_3)_{H_2O} = \varepsilon(\delta^{15}N\text{-}N_2O_5)_{H_2O} = 1000 \times \left({}^{15}\alpha_{N_2O_5/NO_2} - 1\right) \quad (16)$$

Where, γ is the contribution of ·OH formation pathway to NO_3^-, εN is the nitrogen isotope fractionation value. *f*NO_2 is the fraction of NO_2 in the total NOx. $^{18}\alpha NO_2/NO$, $^{18}\alpha OH/H_2O$, $^{18}\alpha N_2O_5/NO_2$ are the oxygen isotope equilibrium fractionation factors between NO_2 and NO, ·OH and H_2O, N_2O_5 and NO_2, respectively. $^{15}\alpha NO_2/NO$ and $^{15}\alpha N_2O_5/NO_2$ are the nitrogen isotope equilibrium fractionation factor between NO_2 and NO, N_2O_5 and NO_2, respectively.

Table 1. The estimation of $\delta^{15}N\text{-}NH_3$ and $\delta^{15}N\text{-}NOx$ from various sources.

Source	$\delta^{15}N\text{-}NH_3$(‰)	References
Biomass burning	17.5±7.8	(Kawashima and Kurahashi, 2011; Xiao et al., 2020)
Coal combustion	-2.5±6.4	(Felix et al., 2013; Pan et al., 2016)
Urban traffic	6.6±2.1	(Walters et al., 2020)
Fertilizer	-28.3±5.8	(Bhattarai et al., 2021; Chang et al., 2016; Felix et al., 2013; Bhattarai et al., 2020)
Livestock	-18.3±7.7	(Bhattarai et al., 2021; Chang et al., 2016; Felix et al., 2013; Bhattarai et al., 2020)
Urban waste	-22.8±3.6	(Bhattarai et al., 2021; Chang et al., 2016)
Source	$\delta^{15}N\text{-}NOx$(‰)	References
Biomass burning	1.04±4.13	(Zong et al., 2017; Fibiger and Hastings, 2016; Zong et al., 2022)
Coal combustion	13.72±4.57	(Zong et al., 2017; Felix et al., 2015; Felix et al., 2012)
Mobile source	-7.25±7.80	(Zong et al., 2017; Walters et al., 2015)
Soil microbial process	-33.77±12.16	(Zong et al., 2017; Felix and Elliott, 2013)

3. Results and discussion

3.1. Concentration and seasonal variation of NH_4^+ and NO_3^-

The concentration of NH_4^+ and NO_3^- in $PM_{2.5}$ was 1.6±1.3 μg m^{-3} and 2.8±3.4 μg m^{-3}, contributed 18.7% and 32.6% to SIA. The concentration of $N\text{-}NH_4^+$ and $N\text{-}NO_3^-$ was 1.2±1.0

μg m^{-3} and 0.6±0.8 μg m^{-3}, contributed 45.8% and 23.2% to TN, respectively; thus, NH_4^+ and NO_3^- were essential part of nitrogen aerosols. NH_4^+ and NO_3^- showed similar seasonal variations with higher concentrations in winter than in summer (**Fig. 1**). During winter the air mass was often dry and cold with low wind speed, which meant the decrease of the atmospheric self-purification capability. In addition, primary combustion sources related to fossil fuel and biomass burning always showed significant increase in North China in winter, which greatly increased the concentration of atmospheric pollutants in Guangzhou by long-range transportation. However, during summer, the air mass from sea was relatively clean with high wind speed facilitating the diffusion of pollutants. Moreover, high temperature in summer was conducive to the decomposition of NH_4NO_3(Song et al., 2008). Thus, the levels of NH_4^+ and NO_3^- were lower in summer. In addition, concentrations of NH_4^+ and NO_3^- in our study, were lower than North China [Beijing(Wu et al., 2019; Fan et al., 2022), Tianjin(Xiang et al., 2022), Shijiazhuang(Xiang et al., 2022), and Harbin(Sun et al., 2021)], East China [Nanchang(Xiao et al., 2020)], and Central China [Wuhan and Changsha(Xiao et al., 2020; Zong et al., 2020)], suggested the level of air pollution in Guangzhou has been alleviated to a certain extent. Therefore, it is necessary to conduct comprehensive study on the emission sources of NH_4^+ and NO_3^- to take more effective measures to mitigate air pollution.

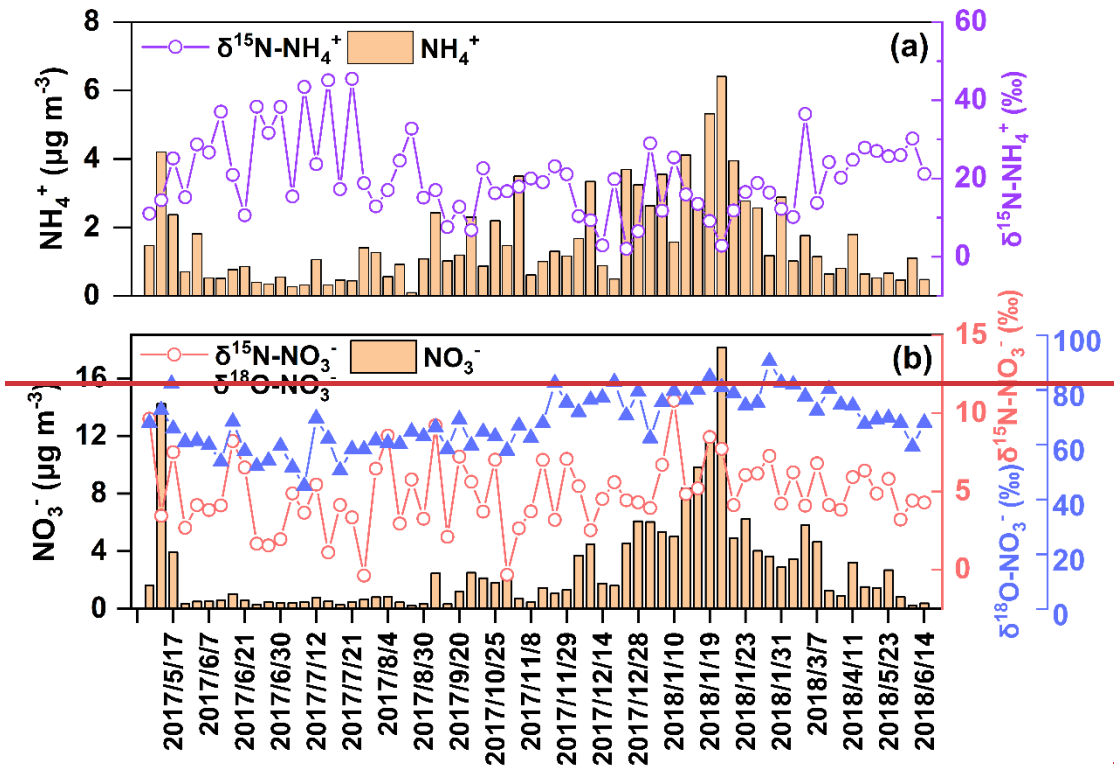

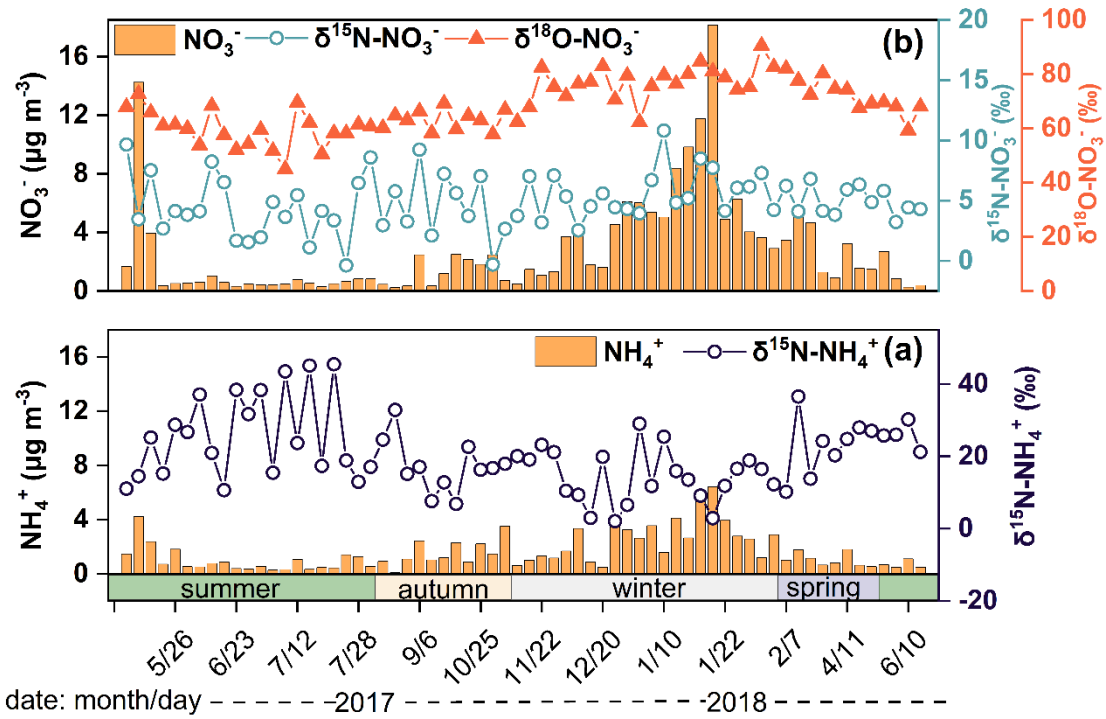

Figure 1. The concentration and $\delta^{15}N$ of NH_4^+ (a) and concentration, $\delta^{15}N$, and $\delta^{18}O$ of NO_3^- (b).

3.2. Characteristic and seasonal variation in $\delta^{15}N$-NH_4^+ and source apportionment of NH_4^+

The $\delta^{15}N$-NH_4^+ values over Guangzhou ranged from 2.1‰ to 45.5‰, with an annual mean of 20.2±10.1‰. In our study, the $\delta^{15}N$-NH_4^+ values were comparable to those at suburban sites (**Fig. S~~1~~2**) such as sites in Japan (22.1±8.3‰, 16.1±6.6‰)(Kawashima and Kurahashi, 2011) and Korea (Jeju Island,17.4±4.9‰)(Kundu et al., 2010) but heavier than those in polluted regions, such as ~~Heshan in Pearl River Delta (PRD)~~ Guangzhou during summer haze(average~~±~~ 7.17‰)(Liu et al., 2018) and Beijing (-37.1‰ to ~~±~~5.8‰)(Pan et al., 2016). $\delta^{15}N$-NH_4^+ values were lower in autumn (17.3‰) and winter (14.4‰) than in spring (22.5‰) and summer (25.7‰), which was similar to the trends in Japan(Kawashima and Kurahashi, 2011).

The seasonal differences in $\delta^{15}N$-NH_4^+ values were significant between warm (summer/spring) and ~~cool~~ cold seasons (winter/~~fall~~ autumn) ($p < 0.05$). The $\delta^{15}N$-NH_4^+ was affected by the ratio of $NH_4^+/(NH_3+NH_4^+)$ (~~**Text S3**~~**Eq. (8) and Fig. S1**). A linear fitting equation was observed between $NH_4^+/(NH_3+NH_4^+)$ and $\delta^{15}N$-NH_4^+, and the absolute value of

the slope (32.4) approximated the isotope equilibrium fractionation value (~~+~~33%) between atmospheric NH_3 and NH_4^+ (**Fig. S~~2~~1**). The linear fitting suggested that the lower the NH_4^+ proportion was, the heavier the δ^{15}N-NH_4^+ value. The lower NH_4^+ level was accordance with higher δ^{15}N-NH_4^+ in summer, which was the opposite of winter. In addition, previous study suggested that the marked variation in δ^{15}N-NH_4^+ values was largely controlled by the emission sources of NH_3, the precursor gas of NH_4^+(Liu et al., 2018). According to the δ^{15}N-NH_4^+ results, the source of NH_4^+ was assigned as biomass burning (27.9±16.4%), coal combustion (16.0±3.9%), vehicles (19.8±5.3%), fertilizer (10.9±6.1%), livestock (12.7±5.8%), and urban waste (11.9±6.1%), shown in **Fig. 2a**.

In our study, non-agriculture sources were the dominators of NH_4^+ (75.6~~1~~%). Unexpectedly, the contribution of biomass burning was the highest. Especially, from late June to July, the contribution of biomass burning enhanced, which possibly resulted from sugarcane leaf burning. The δ^{15}N in sugarcane leaf was as high as 38‰(Martinellia et al., 2002). ~~The δ^{15}N-NH_4^+ released from sugarcane leaf was estimated as 44.1‰ (**SI Text S4**), which coincided with the highest δ^{15}N-NH_4^+ value in July (45.5‰ and 45.1‰).~~ The δ^{15}N of NH_4^+ formed from NH_3 released by sugarcane leaves burning was 44.1‰ (**SI Text S3**), which was consistent with the highest δ^{15}N-NH_4^+ values (45.5‰ and 45.1‰) in July. In PRD, south winds prevail in July and the sampling site is located downwind of sugarcane planting area. Therefore, the air mass to the sampling site might carry the pollutants related to sugarcane leaf burning. K^+ is a typical biomass burning tracer(Cui et al., 2018). Considering the impact of primary emission intensity, [NH_4^+/EC] and [K^+/EC] were used to calculate the correlation coefficient ($r=0.435$, $p < 0.01$), which verified NH_4^+ was influenced by biomass burning. In recent years, biomass burning has been gradually identified as an important source of NH_4^+(Meng et al., 2017; Xiao et al., 2020). The results based on emission inventories showed that the contribution of residential biomass combustion to NH_3 ranged from 33% to 53% in China(Meng et al., 2017). According to δ^{15}N, biomass burning contributed 18% [Harbin, East North China](Sun et al., 2021), 46%[Wuhan, South Central China], 40% [Changsha, South Central China](Xiao et al., 2020), 35% [Nanchang, East China](Xiao et al., 2020), and 23% [Guangzhou, South China](Chen et al., 2022a) to NH_4^+. Particularly, in Guangzhou the contribution of biomass burning in the ground was higher than that in Guangzhou tower with ~~the~~ a height of 488 meters, suggested that the

influence of regional biomass burning(Chen et al., 2022a). Furthermore, ^{7}Be ~~is~~ mainly ~~originated~~ originates from upper atmosphere, whereas ^{210}Pb is derived from terrestrial surface(Jiang et al., 2021b). High level of ^{7}Be observed in ground suggested the sink influence of upper atmosphere. ^{7}Be and ^{210}Pb are chemically stable and with unique sources, which can effectively reflect the transport of continental air mass and the air exchange between stratosphere and troposphere. In our study, the correlation coefficient between NH_4^+ and ^{210}Pb ($r=0.701$, $p < 0.01$) was higher than that between NH_4^+ and ^{7}Be ($r=0.432$, $p < 0.01$), suggested that NH_4^+ was mainly affected by regional emission. Therefore, biomass burning exerted essential influence on NH_4^+ level, which should no longer be ignored.

In addition, with the acceleration of urbanization, combustion sources related to fossil fuels have become the main sources of NH_3. In previous studies, the source of NH_x (NH_3+NH_4^+) was mainly from ~~agriculture~~ agricultural activity due to rough way of farming(Chang et al., 2016; Pan et al., 2020). However, with the improvement of efficient fertilization practices, agricultural NH_3 decreased significantly(Wang et al., 2022). Fossil fuels, such as coal and gasoline, are major energies for production and domestic using, and their contribution to NH_3 has become increasingly important. In North China, fossil fuel combustion contributed 92% to NH_3 during hazes(Zhang et al., 2020; Pan et al., 2016). In previous study of Guangzhou, the contribution of NH_3 from fossil source in ground observations (43%) was higher than the observed in Guangzhou tower (18%), indicated the importance of locally related fossil fuel combustion source(Chen et al., 2022a). In our study, vehicle emission and coal combustion contributed 19.8±5.3% and 16.0±3.9% of NH_4^+ respectively, which was lower than ~~the~~ North China but higher than agricultural sources. The share of NH_3 from vehicle exhaust was estimated to be 18.8% based on the emission factor of NH_3 from on road vehicles in Guangzhou, which was similar to our results(Liu et al., 2014). The selective catalytic reduction process for vehicle can reduce NOx, but increased emission of NH_3, which has confirmed as an important source of NH_3(Heeb et al., 2006; Meng et al., 2017). Despite the efforts of government to promote electric vehicles in recent years, their share is still relatively low (about 5%). As increasing car ownership, this has an important impact on atmospheric NH_3. Coal combustion was the second most important source of fossil combustion after vehicle emissions in our study, although the contribution was lower than in North China(Wu et al., 2019; Zhang et al., 2020;

Pan et al., 2016). The absence of heating in Guangzhou may explain the lower contribution of coal combustion compared to the North. On an annual basis, the contribution of fossil fuel-related combustion sources in our study (35.8%) was comparable to that in North China (37%-52%)(Pan et al., 2018a).

The source contributions of NH_4^+ in our study were compared to other regions, shown in **Fig. S3**. The combustion related sources (biomass burning, coal combustion, and vehicle) have gradually become the dominant source of urban atmospheric NH_3. Biomass burning and vehicle could emit massive carbon monoxide (CO)(Li and Wang, 2007; Wang et al., 2005). In Guangzhou, NH_4^+ was positively related to CO (r=0.637, p < 0.01), which confirmed combustion sources ~~playing~~ played a key role in NH_4^+. From a historical perspective, NH_3 emissions from anthropogenic combustion and industry have been steadily increasing since 1960(Meng et al., 2017). The optimization of energy structure and encouragement of the development of new energy vehicle would be hopeful to reduce NH_3. The results of this study would be conducive to ~~reduce~~ reducing NH_3 scientifically and effectively~~,~~ and would relieve the pressure on the reduction from agricultural source.

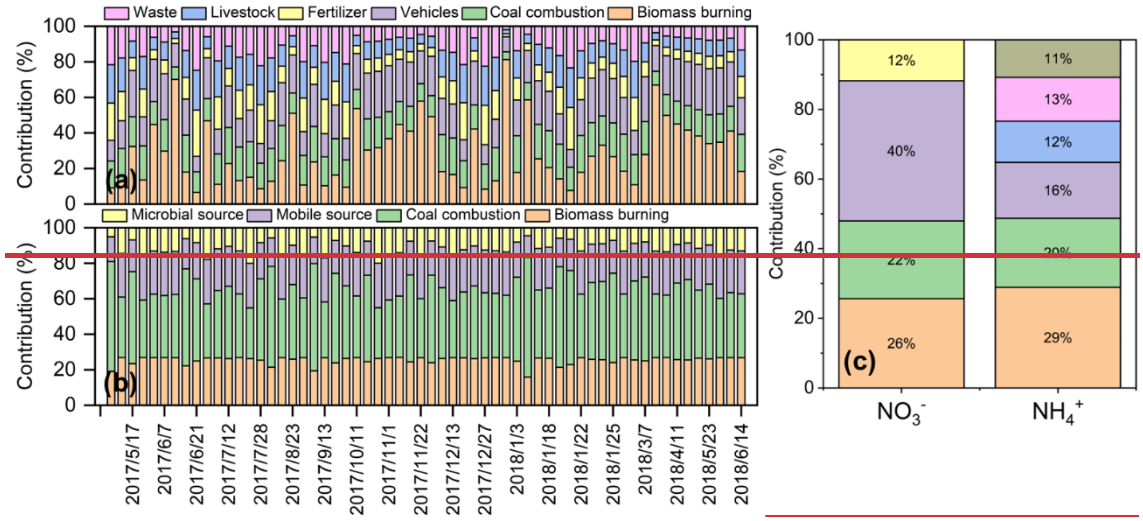

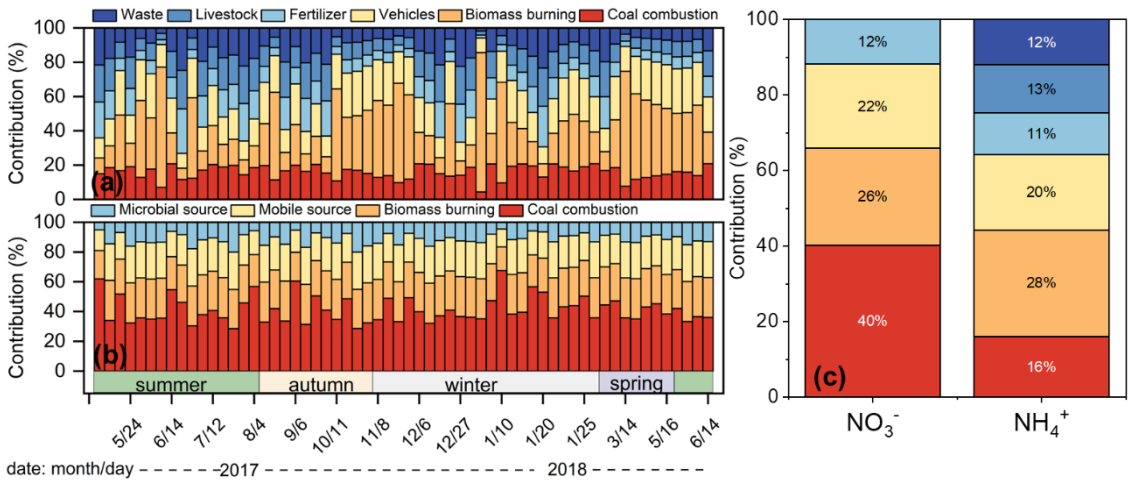

Figure 2. The sources apportionment results of atmospheric NH_4^+ (a) and NO_3^- (b) in Guangzhou, and the comparison of sources results between NH_4^+ and NO_3^- (c).

3.3. Characteristic and seasonal variation in $\delta^{18}O\text{-}NO_3^-$ and $\delta^{15}N\text{-}NO_3^-$ and source apportionment of NO_3^-

3.3.1. Seasonal variation of $\delta^{18}O\text{-}NO_3^-$

The $\delta^{18}O\text{-}NO_3^-$ in Guangzhou was 68.1±9.7‰ (44.9‰ to 90.5‰) comparable to that in precipitation (66.3~~±2.8~~‰, ranging from 33.4‰ to 86.2‰)(Fang et al., 2011), but lower than those regions with weak light intensity, such as Bei~~ChengHuang~~huangcheng Island (~~76.6±8.1‰~~ranging from 49.4‰ to 103.9‰)(Zong et al., 2017) and Bermuda Islands (~~71.1±3.0‰~~cold season 76.9±6.3‰) (Hastings et al., 2003). In this study, $\delta^{18}O\text{-}NO_3^-$ was higher in winter and spring than in summer and autumn, which was similar to the seasonal variation in $\delta^{18}O\text{-}NO_3^-$ in previous studies (Fang et al., 2011; Gobel et al., 2013). On the one hand, $\delta^{18}O\text{-}NO_3^-$ value was associated with the formation pathways of NO_3^-. The results simulated by Bayesian mixing model suggested that the contributions of N_2O_5 channel to NO_3^- were 56.8%, 58.9%, 29.2%, and 27.0% in winter, spring, ~~fall~~autumn, and summer, respectively. The $\delta^{18}O$ value of NO_3^- formed by N_2O_5 channel is higher than that by ·OH pathway (**SI Text S~~5~~2**). The night in cold season was longer than that in warm season, which favored NO_3^- formation through N_2O_5 channel. In addition, the illumination intensity was weakened in cold season compared with that in warm season, which constrained the production of ·OH(Zong et al., 2020; Tan et al., 2019; Wang et al., 2017). Thus, the contribution of the N_2O_5 channel in

cold season was higher than that in warm season. Furthermore, concentration of NO_3^- was high when contribution of N_2O_5 channel enhanced (**Fig. 3**), suggested NO_3^- pollution was related to N_2O_5 hydrolysis pathway. The air mass to Guangzhou was derived from the South China Sea in summer and the North continental region in winter. The higher $\delta^{18}O\text{-}NO_3^-$ and NO_3^- concentration might be affected by long-range and high-altitude transport from North China, which might carry abundant ~~of~~ precursors. Massive NO_3^- could be formed by N_2O_5 hydrolysis at high altitude and transported to the ground. The index of $f(^7Be,^{210}Pb)$ was expressed in **SI Text S1** and could reflect the influence of atmospheric dynamic transport on aerosol pollutants(Jiang et al., 2021b). Generally, air masses with low values of $f(^7Be,^{210}Pb)$ suggested that pollutants were associated with continental surface emission, whereas high $f(^7Be,^{210}Pb)$ were influenced by long-range transport from upper air masses. The contribution of N_2O_5 channel was positively correlated with $f(^7Be,^{210}Pb)$ ($r=0.319$, $p < 0.05$), indicated the long-range transport influence of upper air mass on N_2O_5 channel. For example, on 25 January 2018, the contribution of N_2O_5 channel (nitrate) was 81.1% (3.6 μg m^{-3}), when the upper air mass was from ~~the~~ North China. However, on 7 July 2017, the N_2O_5 channel (nitrate) contributed only 5.7% (0.5 μg m^{-3}) corresponding to the air mass mainly from the South China Sea transported at low-altitude (**Fig. S4**).

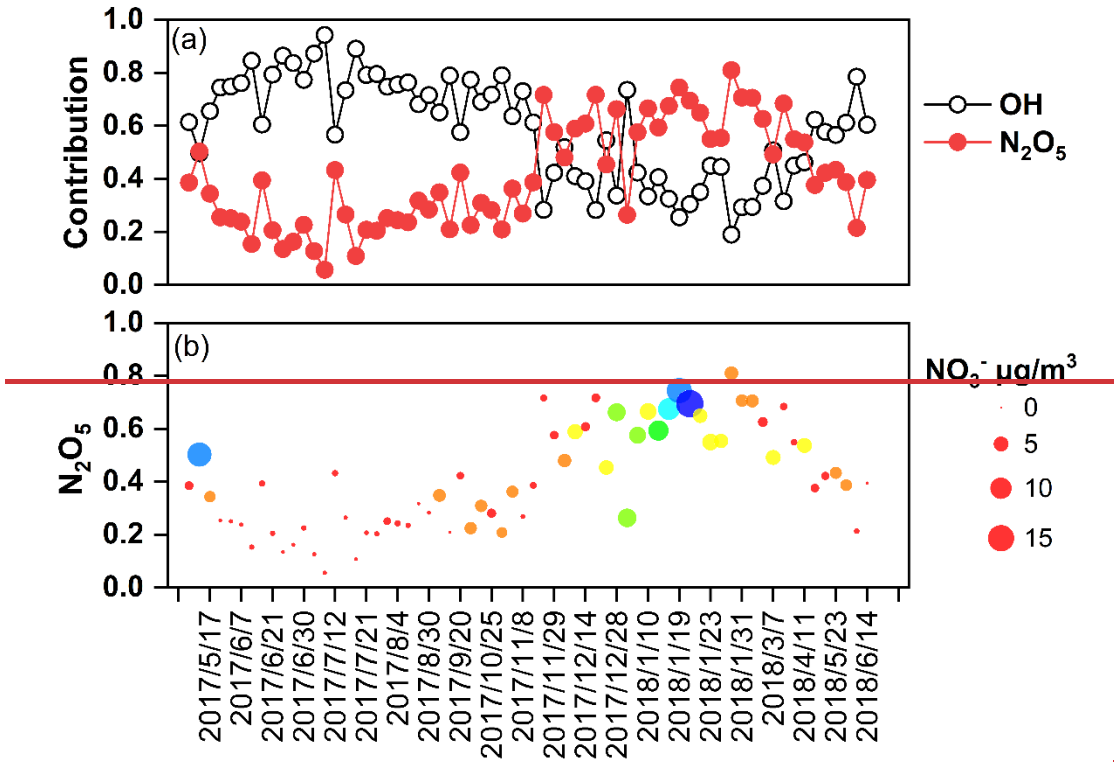

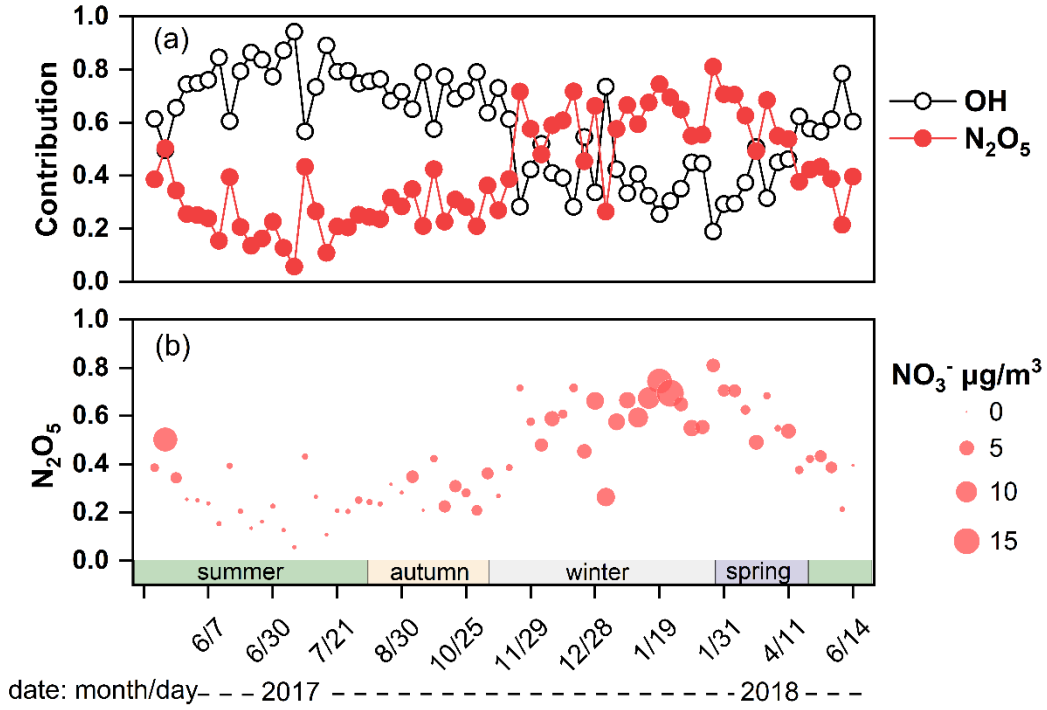

Figure 3. The contribution of the OH radical oxidation and N_2O_5 hydrolysis pathway to NO_3^- (a). The vertical position of dots corresponded to the contribution of N_2O_5 pathway and the size of the dots corresponded to the concentration of NO_3^- (b).

$\delta^{18}O\text{-}NO_3^-$ decreased from 76.7‰ in 2014 to 68.1‰ in 2017-2018(Zong et al., 2020), which indicated that ·OH channel became more important in Guangzhou. The enhanced contribution of ·OH pathway indicated the increasing atmospheric oxidation capacity. In recent years, although the concentration of $PM_{2.5}$ in Guangzhou has significantly decreased, the photochemical pollution caused by high O_3 concentrations was not optimistic(Tan et al., 2019). The O_3 concentration in the PRD showed a fluctuating upward trend from 2013 to 2020; especially in 2017-2018, O_3 concentrations were at high levels (Environmental Status Bulletin of Guangdong Province **Fig. S5**). In our study, the NO_3^- formation pathway inferred from $\delta^{18}O\text{-}NO_3^-$ proved the enhancement of atmospheric oxidation capacity.

3.3.2. Seasonal variation of $\delta^{15}N\text{-}NO_3^-$ and source apportionment of NO_3^-

Seasonal variation of $\delta^{15}N\text{-}NO_3^-$. The $\delta^{15}N\text{-}NO_3^-$ in Guangzhou was 4.9±2.2‰ (-0.4‰ to 10.8‰), which was similar to the wet deposition(Fang et al., 2011). The $\delta^{15}N\text{-}NO_3^-$ was comparable to that from the Northeast United States (6.8‰)(Elliott et al., 2009), and lower

than regions in China, where NO_3^- was predominantly derived from anthropogenic sources, such as Heshan in Guangdong (7.50±3.30‰)(Su et al., 2020), Bei~~ChengHuang~~huangcheng Island (8.2~~0~~±6.2~~0~~‰)(Zong et al., 2017), and Beijing (12.1±3.3‰)(Fan et al., 2022). Nevertheless, the $\delta^{15}N\text{-}NO_3^-$ in this study was significantly higher than those from clean background regions, where NO_3^- was mainly from natural sources, such as the coast of Antarctica (~~-12.4±7.20~~-12.0±15.6‰)(Savarino et al., 2007) and Bermuda (-2.1±1.5‰ warm season, -5.9±3.3‰ ~~cool~~ cold season)(Hastings et al., 2003). The values of $\delta^{15}N\text{-}NO_3^-$ in winter, spring, summer, and autumn were 5.6‰, 5.3‰, 4.4‰, and 4.5‰, respectively. The $\delta^{15}N\text{-}NO_3^-$ in winter and summer showed significant difference ($p < 0.05$). The values of $\delta^{15}N\text{-}NO_3^-$ were influenced by atmospheric processes and emission sources(Elliott et al., 2009). For N_2O_5 channel, NO_3^- is characterized by higher $\delta^{15}N$ values(Freyer et al., 1993; Elliott et al., 2009). The N_2O_5 channel was the predominant formation pathway of NO_3^- in winter, which was in accordance with the seasonal variation in $\delta^{15}N\text{-}NO_3^-$. In addition, the difference in $\delta^{15}N\text{-}NO_3^-$ reflected the variation in the emission source of NO_3^-. $\delta^{15}N$-NOx from coal combustion was relatively high. In winter, the higher $\delta^{15}N\text{-}NO_3^-$ was probably related to long-range transport from North, where coal combustion enhanced in winter.

Source apportionment of NO_3^-. Based on the Bayesian mixing model coupled with $\delta^{15}N\text{-}NO_3^-$, NO_3^- sources were assigned as coal combustion 40.4±8.7%, biomass burning 25.6±2.1%, mobile sources (vehicles) 22.3±3.1%, and microbial process 11.7±3.8%. **Figure 2b** and ~~**Figure**~~ **Fig. S6** showed the source contribution of NO_3^- in Guangzhou and other regions in China, respectively. Compared to earlier periods (2013-2014), the concentration of NO_3^- from vehicle and coal combustion decreased significantly(Zong et al., 2020), which resulted from the stricter vehicle emission standard, promotion of new energy electric vehicles, and ultraclean transformation of coal combustion(Guangdongprovince, 2014; Tang et al., 2019). However, almost all production and domestic segments rely on energy generated from coal combustion, which was still dominant source of NO_3^- in 2017-2018. Coal combustion was affected not only by local emissions but also by external air mass transmission. The contribution of coal combustion was higher in winter than in summer, which probably related to the long-range transportation from the North. Taking 10 January 2018 as an example, the contribution of coal combustion sources to NO_3^- was 67.5%, and the corresponding air mass was from the North

and transmitted to Guangzhou through high altitude. However, the air mass on 26 July 2017 ~~were~~ was mainly from the South China Sea, which was transmitted through low-altitude to Guangzhou. The contribution of coal burning to NO_3^- on 26 July 2017 was 28.5% lower than that on 10 January 2018.

As non-fossil combustion source, biomass burning was also an important source of NO_3^- and accounted for 25.6%. The contribution of biomass burning and vehicle was stable throughout a year. Generally, high intensity biomass burning occurred in winter in Guangdong province (dry season, i.e., from November to March)(Xu et al., 2019). K^+ is a typical tracer of biomass burning. The concentration of K^+ enhanced in winter (0.4μg/m^3) was higher than that in summer (0.2μg/m^3) and autumn (0.2μg/m^3), respectively, indicating enhancement of biomass burning intensity. Also, NO_3^- concentration of biomass burning remarkably enhanced in winter (1.2μg/m^3), and was higher than that in summer (0.4μg/m^3) and autumn (0.3μg/m^3), respectively. However, coal combustion also enhanced in winter due to the demand for heating in North China. Our sampling site was influenced by the air mass with high coal combustion contribution from the North by long-range transportation, which may reduce the contribution of biomass burning relatively. Thus, the contribution of biomass burning showed stable compared with coal combustion. Another non-fossil source is related to soil microbial activity and only contributed 11.7% to NO_3^-, which was unexpectedly lower than the results in earlier periods (2013-2014). Generally, the microorganisms in soil emit NO through nitrification or denitrification, which was affected by the amount of carbon and nitrogen nutrients in soil(Hall and Matson, 1996). In earlier periods, due to the higher level of aerosols, the amount of nutrients settling in soil was also higher, which was exemplified by the observation of dry and wet deposition in Guangzhou(He et al., 2022; Zheng et al., 2020). In addition, the reduction of cultivated land from 2013 to 2018 might also reduce the contribution of microbial source emissions. Therefore, emissions from natural sources were also influenced by human activities to some extent. The contribution of microbial process was higher in summer than in winter. In summer, higher RH and temperature were favorable for the intense activity of soil microorganisms(Zong et al., 2017). The contributions of microbial processes to NO_3^- also decreased in winter compared with summer at regional background sites and five Chinese megacities, including Guangzhou(Zong et al., 2017; Zong et al., 2020).

The sources comparison between NO_3^- and NH_4^+ was shown in **Fig. 2c**. Coal combustion, biomass burning, and vehicles were three significant sources of NO_3^- and NH_4^+. Coal combustion and biomass burning were the dominant sources of NO_3^- and NH_4^+, respectively. The vehicles were also an important source of atmospheric inorganic Nr contributed to 22.3% and 19.8% ~~to~~ of NO_3^- and NH_4^+, respectively. Recently, the government has actively taken many measures to reduce the pollution from vehicles, such as stricter automobile emission standards and the promotion of new energy vehicles. However, due to the large vehicle ownership base, the pollutants emitted from vehicles are not optimistic. In addition, vehicles emissions could contribute half of the fresh secondary organic aerosol in urban environment(Zhang et al., 2022; Zhao et al., 2022a).

4. Conclusions

A year-long field observation was conducted in Guangzhou to clarify the atmospheric fate of inorganic nitrogen aerosol. Inorganic nitrogen species were the most essential component of TN including NH_4^+ (45.8%) and NO_3^- (23.2%), which are also dominant components of SIA and play a key role in China haze. The $\delta^{15}N$ is a powerful tool to quantify the source contribution of NH_4^+ and NO_3^-, which suggested that anthropogenic combustion sources (coal combustion, biomass burning, and vehicles) were the dominant sources.

Anthropogenic combustion sources contributed 63.2% to NH_4^+ higher than agricultural sources (23.6%). NH_3 largely facilitates the formation of sulfate and nitrate. Meanwhile, sulfate and nitrate promote each other with positive feedback effect, which could trigger haze. In megacities of China, the focus of NH_3 reduction should be on anthropogenic combustion sources, especially on biomass burning, which might be responsible for the lag of the decline in the deposition of air pollutions behind the reduction in emission(Zhao et al., 2022b). In addition, anthropogenic combustion sources accounted for 88.3% of NO_3^-. Coal combustion and vehicles contributed 40.4% and 22.3% to NO_3^-, respectively. Despite a series of measures to reduce emissions of NOx, fossil fuels, as the main energy for production and living, will still inevitably emit a large amount of NOx. Our results emphasized that the emission of atmospheric inorganic nitrogen is largely related to anthropogenic combustion sources. The

development and promotion of clean energy and efficient use of biomass are conducive to the deep reduction of atmospheric nitrogen.

Data availability

The original data of this research (stable nitrogen isotopes and inorganic nitrogen concentrations) are available at Mendeley data (Li and Li, 2023). The Iso Source model was downloaded from Environmental Protection Agency, via their website: https://www.epa.gov/sites/default/files/2015-11/isosourcev1_3_1.zip.

Author contributions

Funding acquisition: Jun Li

Investigation: Tingting Li, Zeyu Sun, and Hongxing Jiang

Methodology: Tingting Li, Zeyu Sun, Hongxing Jiang, Jun Li, and Chongguo Tian

Project Administration: Jun Li

Resources: Jun Li, Chongguo Tian, and Gan Zhang

Software: Tingting Li, Zeyu Sun, and Chongguo Tian

Validation: Tingting Li and Jun Li

Writing – original draft: Tingting Li

Writing – review & editing: Jun Li

Competing interests

The authors declare that they have no conflict of interest.

Financial support

This study was supported by the Natural Science Foundation of China (NSFC; Nos. (41977177), Guangdong Basic and Applied Basic Research Foundation (2021A1515011456), Guangdong Foundation for Program of Science and Technology Research (Grant No. 2019B121205006 and 2020B1212060053).

References

Baskaran, M., K., B. S., and F., M. D.: Oxygen isotope dynamics of atmospheric nitrate and its precursor molecules. In Handbook of Environmental Isotope Geochemistry., Springer-Verlag Berlin Heidelberg2011.

Bhattarai, H., Zhang, Y. L., Pavuluri, C. M., Wan, X., Wu, G., Li, P., Cao, F., Zhang, W., Wang, Y., Kang, S., Ram, K., Kawamura, K., Ji, Z., Widory, D., and Cong, Z.: Nitrogen speciation and isotopic composition of aerosols collected at Himalayan Forest (3326 m a.s.l.): seasonality, sources, and implications, Environ. Sci. Technol., 53, 12247-12256, https://doi.org/10.1021/acs.est.9b03999, 2019.

Bhattarai, N., Wang, S., Pan, Y., Xu, Q., Zhang, Y., Chang, Y., and Fang, Y.: δ^{15}N-stable isotope analysis of NHx : An overview on analytical measurements, source sampling and its source apportionment, Front. Environ. Sci. Eng., 15, 126, https://doi.org/10.1007/s11783-021-1414-6, 2021.

Bhattarai, N., Wang, S., Xu, Q., Dong, Z., Chang, X., Jiang, Y., and Zheng, H.: Sources of gaseous NH_3 in urban Beijing from parallel sampling of NH_3 and NH_4^+, their nitrogen isotope measurement and modeling, Sci. Total Environ., 747, 141361, https://doi.org/10.1016/j.scitotenv.2020.141361, 2020.

Breemen, N. V.: Nitrogen cycle natural organic tendency, Nature, 415, https://doi.org/10.1038/415381a, 2002.

Chang, Y., Liu, X., Deng, C., Dore, A. J., and Zhuang, G.: Source apportionment of atmospheric ammonia before, during, and after the 2014 APEC summit in Beijing using stable nitrogen isotope signatures, Atmos. Chem. Phys., 16, 11635-11647, https://doi.org/10.5194/acp-16-11635-2016, 2016.

Chen, Z., Pei, C., Liu, J., Zhang, X., Ding, P., Dang, L., Zong, Z., Jiang, F., Wu, L., Sun, X., Zhou, S., Zhang, Y., Zhang, Z., Zheng, J., Tian, C., Li, J., and Zhang, G.: Non-agricultural source dominates the ammonium aerosol in the largest city of South China based on the vertical δ^{15}N measurements, Sci. Total Environ., 848, 157750, https://doi.org/10.1016/j.scitotenv.2022.157750, 2022a.

Chen, Z. L., Song, W., Hu, C. C., Liu, X. J., Chen, G. Y., Walters, W. W., Michalski, G., Liu, C. Q., Fowler, D., and Liu, X. Y.: Significant contributions of combustion-related sources to ammonia emissions, Nat. Commun., 13, 7710, https://doi.org/10.1038/s41467-022-35381-4, 2022b.

Cui, M., Chen, Y., Zheng, M., Li, J., Tang, J., Han, Y., Song, D., Yan, C., Zhang, F., Tian, C., and Zhang, G.: Emissions and characteristics of particulate matter from rainforest burning in the Southeast Asia, Atmos. Environ., 191, 194-204, https://doi.org/10.1016/j.atmosenv.2018.07.062, 2018.

Dunne, E. M., Gordon, H., Kürten, A., Almeida, J., Duplissy, J., Williamson, C., Ortega, I. K., Pringle, K. J., Adamov, A., and Schobesberger, S.: Global atmospheric particle formation from cern cloud measurements, Science, 354, 1119-1123, https://doi.org/10.1126/science.aaf2649, 2016.

Elliott, E. M., Kendall, C., Wankel, S. D., Burns, D. A., Boyer, E. W., Harlin, K., Bain, D. J., and Butler, T. J.: Nitrogen isotopes as indicators of NOx source contributions to atmospheric nitrate deposition across the midwestern and Northeastern United States, Environ. Sci. Technol., 41, 7661-7667, https://doi.org/10.1021/es070898t, 2007.

Elliott, E. M., Kendall, C., Boyer, E. W., Burns, D. A., Lear, G. G., Golden, H. E., Harlin, K., Bytnerowicz, A., Butler, T. J., and Glatz, R.: Dual nitrate isotopes in dry deposition: Utility for partitioning NOx source contributions to landscape nitrogen deposition, J. Geophys. Res. , 114, https://doi.org/10.1029/2008JG000889, 2009.

Fan, M.-Y., Zhang, Y.-L., Hong, Y., Lin, Y.-C., Zhao, Z.-Y., Cao, F., Sun, Y., Guo, H., and Fu, P.: Vertical differences of nitrate sources in urban boundary layer based on tower measurements, Environ. Sci. Technol. Lett., 2c00600, https://doi.org/10.1021/acs.estlett.2c00600, 2022.

Fan, M. Y., Zhang, Y. L., Lin, Y. C., Cao, F., Zhao, Z. Y., Sun, Y., Qiu, Y., Fu, P., and Wang, Y.: Changes of emission sources to nitrate aerosols in Beijing after the clean air actions: evidence from dual isotope compositions, J. Geophys. Res.: Atmos., 125, 031998, https://doi.org/10.1029/2019jd031998, 2020.

Fang, Y. T., Koba, K., Wang, X. M., Wen, D. Z., Li, J., Takebayashi, Y., Liu, X. Y., and Yoh, M.: Anthropogenic imprints on nitrogen and oxygen isotopic composition of precipitation nitrate in a nitrogen-polluted city in southern China, Atmos. Chem. Phys., 11, 1313-1325, https://doi.org/10.5194/acp-11-1313-2011, 2011.

Felix, J. D. and Elliott, E. M.: The agricultural history of human-nitrogen interactions as recorded in ice core $\delta^{15}N$-NO_3^-, Geophys. Res. Lett., 40, 1642-1646, https://doi.org/10.1002/grl.50209, 2013.

Felix, J. D., Elliott, E. M., and Shaw, S. L.: Nitrogen isotopic composition of coal-fired power plant NOx: influence of emission controls and implications for global emission inventories, Environ. Sci. Technol., 46, 3528-3535, https://doi.org/10.1021/es203355v, 2012.

Felix, J. D., Elliott, E. M., Gish, T. J., McConnell, L. L., and Shaw, S. L.: Characterizing the isotopic composition of atmospheric ammonia emission sources using passive samplers and a combined oxidation-bacterial denitrifier approach, Rapid Commun. Mass Spectrom., 27, 2239-2246, https://doi.org/10.1002/rcm.6679, 2013.

Felix, J. D., Elliott, E. M., Avery, G. B., Kieber, R. J., Mead, R. N., Willey, J. D., and Mullaugh, K. M.: Isotopic composition of nitrate in sequential Hurricane Irene precipitation samples: Implications for changing NOx sources, Atmos. Environ., 106, 191-195, https://doi.org/10.1016/j.atmosenv.2015.01.075, 2015.

Fibiger, D. L. and Hastings, M. G.: First Measurements of the Nitrogen Isotopic Composition of NOx from Biomass Burning, Environ. Sci. Technol., 50, 11569-11574, https://doi.org/10.1021/acs.est.6b03510, 2016.

Freyer, H. D., Kley, D., Volz-Thomas, A., and Kobel, K.: On the interaction of isotopic exchange processes with photochemical reactions in atmospheric oxides of nitrogen, J. Geophys. Res. , 98, 14,791-714,796, https://doi.org/10.1029/93JD00874, 1993.

Fu, X., Wang, S., Xing, J., Zhang, X., Wang, T., and Hao, J.: Increasing ammonia concentrations reduce the effectiveness of particle pollution control achieved via SO_2 and NO_X emissions reduction in East China, Environ. Sci. Technol. Lett., 4, 221-227, https://doi.org/10.1021/acs.estlett.7b00143, 2017.

Galloway, J. N., Dentener, F. J., Capone, D. G., Boyer, E. W., Howarth, R. W., Seitzinger, S. P., Asner, G. P., Cleveland, C. C., Green, P. A., Holland, E. A., Karl, D. M., Michaels, A. F., Porter, J. H., Townsend, A. R., and VörO¨smarty, C. J.: Nitrogen cycles past present and future, Biogeochemistry, 70, 153-226, https://doi.org/10.1007/s10533-004-0370-0, 2004.

Gobel, A. R., Altieri, K. E., Peters, A. J., Hastings, M. G., and Sigman, D. M.: Insights into anthropogenic nitrogen deposition to the North Atlantic investigated using the isotopic composition of aerosol and rainwater nitrate, Geophys. Res. Lett., 40, 5977-5982, https://doi.org/10.1002/2013gl058167, 2013.

Action Plan for Air Pollution Control of Guangdong Province (2014-2017): http://www.gd.gov.cn/gkmlpt/content/0/142/mpost_142687.html, last access: February 14, 2014.

Hall, S. J. and Matson, P. A.: NOx emissions from soil: implications for air quality modeling in agricultural regions, Annu. Rev. Energy Environ., 21, 311-346, https://doi.org/10.1146/annurev.energy.21.1.311, 1996.

Hastings, M. G., Sigman, D. M., and Lipschultz, F.: Isotopic evidence for source changes of nitrate in rain at Bermuda, J. Geophys. Res.: Atmos., 108, 1-12, https://doi.org/10.1029/2003jd003789, 2003.

He, S., Huang, M., Zheng, L., Chang, M., Chen, W., Xie, Q., and Wang, X.: Seasonal variation of transport pathways and potential source areas at high inorganic nitrogen wet deposition sites in southern China, J. Environ. Sci. (China), 114, 444-453, https://doi.org/10.1016/j.jes.2021.12.024, 2022.

Heaton, T. H. E., Spiro, B., and Robertson, S. M. C.: Potential canopy influences on the isotopic composition of nitrogen and sulphur in atmospheric deposition, Oecologia, 109, 600-607, 1997.

Heeb, N. V., Forss, A.-M., Brühlmann, S., Lüscher, R., Saxer, C. J., and Hug, P.: Three-way catalyst-induced formation of ammonia—velocity- and acceleration-dependent emission factors, Atmos. Environ., 40, 5986-5997, https://doi.org/10.1016/j.atmosenv.2005.12.035, 2006.

585 Hodas, N., Sullivan, A. P., Skog, K., Keutsch, F. N., Collett, J. L., Jr., Decesari, S., Facchini, M. C., Carlton, A.
586 G., Laaksonen, A., and Turpin, B. J.: Aerosol liquid water driven by anthropogenic nitrate: implications for
587 lifetimes of water-soluble organic gases and potential for secondary organic aerosol formation, Environ. Sci.
588 Technol., 48, 11127-11136, https://doi.org/10.1021/es5025096, 2014.
589 Holland, E. A., Dentener, F. J., Braswell, B. H., and Sulzman, J. M.: Contemporary and pre-industrial global
590 reactive nitrogen budgets, Biogeochemistry, 46, 7-43, https://doi.org/10.1007/BF01007572, 1999.
591 Huang, S., Elliott, E. M., Felix, J. D., Pan, Y., Liu, D., Li, S., Li, Z., Zhu, F., Zhang, N., Fu, P., and Fang, Y.:
592 Seasonal pattern of ammonium ^{15}N natural abundance in precipitation at a rural forested site and implications
593 for NH_3 source partitioning, Environ. Pollut., 247, 541-549, https://doi.org/10.1016/j.envpol.2019.01.023,
594 2019.
595 Huang, Z., Wang, S., Zheng, J., Yuan, Z., Ye, S., and Kang, D.: Modeling inorganic nitrogen deposition in
596 Guangdong province, China, Atmos. Environ., 109, 147-160,
597 https://doi.org/10.1016/j.atmosenv.2015.03.014, 2015.
598 Jiang, H., Li, J., Sun, R., Tian, C., Tang, J., Jiang, B., Liao, Y., Chen, C., and Zhang, G.: Molecular dynamics and
599 light absorption properties of atmospheric dissolved organic matter, Environ. Sci. Technol., 55, 10268-10279,
600 https://doi.org/10.1021/acs.est.1c01770, 2021a.
601 Jiang, H., Li, J., Sun, R., Liu, G., Tian, C., Tang, J., Cheng, Z., Zhu, S., Zhong, G., Ding, X., and Zhang, G.:
602 Determining the sources and transport of brown carbon using radionuclide tracers and modeling, J. Geophys.
603 Res.: Atmos., 126, e2021JD034616, https://doi.org/10.1029/2021jd034616, 2021b.
604 Johnston, J. C. and Thiemens, M. H.: The isotopic composition of tropospheric ozone in three environments, J.
605 Geophys. Res.: Atmos., 102, 25395-25404, https://doi.org/10.1029/97jd02075, 1997.
606 Kang, Y., Liu, M., Song, Y., Huang, X., Yao, H., Cai, X., Zhang, H., Kang, L., Liu, X., Yan, X., He, H., Zhang,
607 Q., Shao, M., and Zhu, T.: High-resolution ammonia emissions inventories in China from 1980 to 2012,
608 Atmos. Chem. Phys., 16, 2043-2058, https://doi.org/10.5194/acp-16-2043-2016, 2016.
609 Kawashima, H. and Kurahashi, T.: Inorganic ion and nitrogen isotopic compositions of atmospheric aerosols at
610 Yurihonjo, Japan: implications for nitrogen sources, Atmos. Environ., 45, 6309-6316,
611 https://doi.org/10.1016/j.atmosenv.2011.08.057, 2011.
612 Kundu, S., Kawamura, K., and Lee, M.: Seasonal variation of the concentrations of nitrogenous species and their
613 nitrogen isotopic ratios in aerosols at Gosan, Jeju Island: Implications for atmospheric processing and source
614 changes of aerosols, J. Geophys. Res. , 115, https://doi.org/10.1029/2009jd013323, 2010.
615 Li, T. and Li, J.: High contribution of anthropogenic combustion sources to atmospheric inorganic reactive
616 nitrogen in south China evidenced by isotopes, Mendeley data [data set],
617 https://doi.org/10.17632/yck5xy22w2.1, 2023.
618 Li, X. H. and Wang, S. X.: Particulate and trace gas emissions from open burning of wheat straw and corn stover
619 in China, Environ. Sci. Technol., 41, 6052-6058, https://doi.org/10.1021/es0705137, 2007.
620 Liao, B., Wu, D., Chang, Y., Lin, Y., Wang, S., and Li, F.: Characteristics of particulate SO_4^{2-}, NO_3^-, NH_4^+, and
621 related gaseous pollutants in Guangzhou (in Chinese), Acta Sci. Circumst., 34, 1551-1559,
622 https://doi.org/10.13671/j.hjkxxb.2014.0218, 2014.
623 Liu, J., Ding, P., Zong, Z., Li, J., Tian, C., Chen, W., Chang, M., Salazar, G., Shen, C., Cheng, Z., Chen, Y., Wang,
624 X., Szidat, S., and Zhang, G.: Evidence of rural and suburban sources of urban haze formation in China: a
625 case study from the Pearl River Delta region, J. Geophys. Res.: Atmos., 123, 4712-4726,
626 https://doi.org/10.1029/2017jd027952, 2018.
627 Liu, T., Wang, X., Wang, B., Ding, X., Deng, W., Lü, S., and Zhang, Y.: Emission factor of ammonia (NH_3) from
628 on-road vehicles in China: tunnel tests in urban Guangzhou, Environ. Res. Lett., 9, 064027,

https://doi.org/10.1088/1748-9326/9/6/064027, 2014.
Liu, Y., Zhang, Y., Lian, C., Yan, C., Wang, Y., Ge, M., He, H., and Kulmala, M.: The promotion effect of nitrous acid on aerosol formation in wintertime in Beijing: the possible contribution of traffic-related emissions, Atmos. Chem. Phys., 20, 13023–13040, https://doi.org/10.5194/acp-20-13023-2020, 2020.
Liu, Y., Feng, Z., Zheng, F., Bao, X., Liu, P., Ge, Y., Zhao, Y., Jiang, T., Liao, Y., Zhang, Y., Fan, X., Yan, C., Chu, B., Wang, Y., Du, W., Cai, J., Bianchi, F., Petäjä, T., Mu, Y., He, H., and Kulmala, M.: Ammonium nitrate promotes sulfate formation through uptake kinetic regime, Atmos. Chem. Phys., 21, 13269–13286, https://doi.org/10.5194/acp-21-13269-2021, 2021.
Martinellia, L. A., Camargoa, P. B., Laraa, L. B. L. S., Victoriaa, R. L., and Artaxo, P.: Stable carbon and nitrogen isotopic composition of bulk aerosol particles in a C4 plant landscape of southeast Brazil, Atmos. Environ., 36, 2427–2432, https://doi.org/10.1016/S1352-2310(01)00454-X, 2002.
Meng, W., Zhong, Q., Yun, X., Zhu, X., Huang, T., Shen, H., Chen, Y., Chen, H., Zhou, F., Liu, J., Wang, X., Zeng, E. Y., and Tao, S.: Improvement of a global high-resolution ammonia emission inventory for combustion and industrial sources with new data from the residential and transportation sectors, Environ. Sci. Technol., 51, 2821-2829, https://doi.org/10.1021/acs.est.6b03694, 2017.
Meng, Z., Xu, X., Lin, W., Ge, B., Xie, Y., Song, B., Jia, S., Zhang, R., Peng, W., Wang, Y., Cheng, H., Yang, W., and Zhao, H.: Role of ambient ammonia in particulate ammonium formation at a rural site in the North China Plain, Atmos. Chem. Phys., 18, 167-184, https://doi.org/10.5194/acp-18-167-2018, 2018.
Michalski, G., Bhattacharya, S. K., and Girsch, G.: NOx cycle and the tropospheric ozone isotope anomaly: an experimental investigation, Atmos. Chem. Phys., 14, 4935-4953, https://doi.org/10.5194/acp-14-4935-2014, 2014.
Pan, Y., Tian, S., Liu, D., Fang, Y., Zhu, X., Gao, M., Gao, J., Michalski, G., and Wang, Y.: Isotopic evidence for enhanced fossil fuel sources of aerosol ammonium in the urban atmosphere, Environ. Pollut., 238, 942-947, https://doi.org/10.1016/j.envpol.2018.03.038, 2018a.
Pan, Y., Tian, S., Liu, D., Fang, Y., Zhu, X., Zhang, Q., Zheng, B., Michalski, G., and Wang, Y.: Fossil fuel combustion-related emissions dominate atmospheric ammonia sources during severe haze episodes: evidence from ^{15}N-stable isotope in size-resolved aerosol ammonium, Environ. Sci. Technol., 50, 8049-8056, https://doi.org/10.1021/acs.est.6b00634, 2016.
Pan, Y., Tian, S., Liu, D., Fang, Y., Zhu, X., Gao, M., Wentworth, G. R., Michalski, G., Huang, X., and Wang, Y.: Source Apportionment of Aerosol Ammonium in an Ammonia-Rich Atmosphere: An Isotopic Study of Summer Clean and Hazy Days in Urban Beijing, J. Geophys. Res.: Atmos., 123, 5681-5689, https://doi.org/10.1029/2017jd028095, 2018b.
Pan, Y., Gu, M., He, Y., Wu, D., Liu, C., Song, L., Tian, S., Lü, X., Sun, Y., Song, T., Walters, W. W., Liu, X., Martin, N. A., Zhang, Q., Fang, Y., Ferracci, V., and Wang, Y.: Revisiting the concentration observations and source apportionment of atmospheric ammonia, Adv. Atmos. Sci., 37, 933-938, https://doi.org/10.1007/s00376-020-2111-2, 2020.
Qu, K., Wang, X., Xiao, T., Shen, J., Lin, T., Chen, D., He, L. Y., Huang, X. F., Zeng, L., Lu, K., Ou, Y., and Zhang, Y.: Cross-regional transport of $PM_{2.5}$ nitrate in the Pearl River Delta, China: Contributions and mechanisms, Sci. Total Environ., 753, 142439, https://doi.org/10.1016/j.scitotenv.2020.142439, 2021.
Savarino, J., Kaiser, J., Morin, S., Sigman, D. M., and Thiemens, M. H.: Nitrogen and oxygen isotopic constraints on the origin of atmospheric nitrate in coastal Antarctica, Atmos. Chem. Phys., 7, 1925–1945, https://doi.org/10.5194/acp-7-1925-2007, 2007.
Song, W., Liu, X. Y., Hu, C. C., Chen, G. Y., Liu, X. J., Walters, W. W., Michalski, G., and Liu, C. Q.: Important contributions of non-fossil fuel nitrogen oxides emissions, Nat. Commun., 12, 243,

https://doi.org/10.1038/s41467-020-20356-0, 2021.
Song, Y., Dai, W., Wang, X., Cui, M., Su, H., Xie, S., and Zhang, Y.: Identifying dominant sources of respirable suspended particulates in Guangzhou, China, Environ. Eng. Sci., 25, 959-968, https://doi.org/10.1089/ees.2007.0146, 2008.
Su, T., Li, J., Tian, C., Zong, Z., Chen, D., and Zhang, G.: Source and formation of fine particulate nitrate in South China: Constrained by isotopic modeling and online trace gas analysis, Atmos. Environ., 231, https://doi.org/10.1016/j.atmosenv.2020.117563, 2020.
Sun, X., Zong, Z., Li, Q., Shi, X., Wang, K., Lu, L., Li, B., Qi, H., and Tian, C.: Assessing the emission sources and reduction potential of atmospheric ammonia at an urban site in Northeast China, Environ. Res., 198, 111230, https://doi.org/10.1016/j.envres.2021.111230, 2021.
Tan, Z., Lu, K., Jiang, M., Su, R., Wang, H., Lou, S., Fu, Q., Zhai, C., Tan, Q., Yue, D., Chen, D., Wang, Z., Xie, S., Zeng, L., and Zhang, Y.: Daytime atmospheric oxidation capacity in four Chinese megacities during the photochemically polluted season: a case study based on box model simulation, Atmos. Chem. Phys., 19, 3493–3513, https://doi.org/10.5194/acp-19-3493-2019, 2019.
Tang, L., Qu, J., Mi, Z., Bo, X., Chang, X., Anadon, L. D., Wang, S., Xue, X., Li, S., Wang, X., and Zhao, X.: Substantial emission reductions from Chinese power plants after the introduction of ultra-low emissions standards, Nat. Energy, 4, 929-938, https://doi.org/10.1038/s41560-019-0468-1, 2019.
Urey, H. C.: The thermodynamic properties of isotopic substances, J. Chem. Soc., 562-581, https://doi.org/10.1039/jr9470000562, 1947.
Walters, W. W. and Michalski, G.: Theoretical calculation of oxygen equilibrium isotope fractionation factors involving various NOy molecules, OH, and H_2O and its implications for isotope variations in atmospheric nitrate, Geochim. Cosmochim. Ac., 191, 89–101 https://doi.org/10.1016/j.gca.2016.06.039, 2016.
Walters, W. W., Simonini, D. S., and Michalski, G.: Nitrogen isotope exchange between NO and NO_2 and its implications for $\delta^{15}N$ variations in tropospheric NOx and atmospheric nitrate, Geophys. Res. Lett., 43, 440-448, https://doi.org/10.1002/2015gl066438, 2016.
Walters, W. W., Tharp, B. D., Fang, H., Kozak, B. J., and Michalski, G.: Nitrogen Isotope Composition of Thermally Produced NOx from Various Fossil-Fuel Combustion Sources, Environ. Sci. Technol., 49, 11363-11371, https://doi.org/10.1021/acs.est.5b02769, 2015.
Walters, W. W., Song, L., Chai, J., Fang, Y., Colombi, N., and Hastings, M. G.: Characterizing the spatiotemporal nitrogen stable isotopic composition of ammonia in vehicle plumes, Atmos. Chem. Phys., 20, 11551-11567, https://doi.org/10.5194/acp-20-11551-2020, 2020.
Wang, C., Duan, J., Ren, C., Liu, H., Reis, S., Xu, J., and Gu, B.: Ammonia emissions from croplands decrease with farm size in China, Environ. Sci. Technol., 56, 9915-9923, https://doi.org/10.1021/acs.est.2c01061, 2022.
Wang, T., Xue, L., Brimblecombe, P., Lam, Y. F., Li, L., and Zhang, L.: Ozone pollution in China: a review of concentrations, meteorological influences, chemical precursors, and effects, Sci. Total Environ., 575, 1582-1596, https://doi.org/10.1016/j.scitotenv.2016.10.081, 2017.
Wang, X., Carmichael, G., Chen, D., Tang, Y., and Wang, T.: Impacts of different emission sources on air quality during March 2001 in the Pearl River Delta (PRD) region, Atmos. Environ., 39, 5227-5241, https://doi.org/10.1016/j.atmosenv.2005.04.035, 2005.
Wang, X., Wu, Z., Shao, M., Fang, Y., Zhang, L., Chen, F., Chan, P.-w., Fan, Q., Wang, Q., Zhu, S., and Bao, R.: Atmospheric nitrogen deposition to forest and estuary environments in the Pearl River Delta region, southern China, Tellus B: Chem. Phys. Meteorol., 65, https://doi.org/10.3402/tellusb.v65i0.20480, 2013.
Wedin, D. A. and Tilman, D.: Influence of nitrogen loading and species composition on the carbon balance of

grasslands, Science, 274, https://doi.org/10.1126/science.274.5293.1720, 1996.
Wu, L., Ren, H., Wang, P., Chen, J., Fang, Y., Hu, W., Ren, L., Deng, J., Song, Y., Li, J., Sun, Y., Wang, Z., Liu, C.-Q., Ying, Q., and Fu, P.: Aerosol ammonium in the urban boundary layer in Beijing: insights from nitrogen isotope ratios and simulations in summer 2015, Environ. Sci. Technol. Lett., 6, 389-395, https://doi.org/10.1021/acs.estlett.9b00328, 2019.
Xiang, Y.-K., Dao, X., Gao, M., Lin, Y.-C., Cao, F., Yang, X.-Y., and Zhang, Y.-L.: Nitrogen isotope characteristics and source apportionment of atmospheric ammonium in urban cities during a haze event in Northern China Plain, Atmos. Environ., 269, 118800, https://doi.org/10.1016/j.atmosenv.2021.118800, 2022.
Xiao, H. W., Wu, J. F., Luo, L., Liu, C., Xie, Y. J., and Xiao, H. Y.: Enhanced biomass burning as a source of aerosol ammonium over cities in central China in autumn, Environ. Pollut., 266, 115278, https://doi.org/10.1016/j.envpol.2020.115278, 2020.
Xu, Y., Huang, Z., Jia, G., Fan, M., Cheng, L., Chen, L., Shao, M., and Zheng, J.: Regional discrepancies in spatiotemporal variations and driving forces of open crop residue burning emissions in China, Sci. Total Environ., 671, 536-547, https://doi.org/10.1016/j.scitotenv.2019.03.199, 2019.
Yang, Y., Li, P., He, H., Zhao, X., Datta, A., Ma, W., Zhang, Y., Liu, X., Han, W., Wilson, M. C., and Fang, J.: Long-term changes in soil pH across major forest ecosystems in China, Geophys. Res. Lett., 42, 933-940, https://doi.org/10.1002/2014gl062575, 2015.
Yu, X., Shen, L., Hou, X., Yuan, L., Pan, Y., An, J., and Yan, S.: High-resolution anthropogenic ammonia emission inventory for the Yangtze River Delta, China, Chemosphere, 251, 126342, https://doi.org/10.1016/j.chemosphere.2020.126342, 2020.
Zhang, Z., Zeng, Y., Zheng, N., Luo, L., Xiao, H., and Xiao, H.: Fossil fuel-related emissions were the major source of NH_3 pollution in urban cities of northern China in the autumn of 2017, Environ. Pollut., 256, 113428, https://doi.org/10.1016/j.envpol.2019.113428, 2020.
Zhang, Z., Zhu, W., Hu, M., Wang, H., Tang, L., Hu, S., Shen, R., Yu, Y., Song, K., Tan, R., Chen, Z., Chen, S., Canonaco, F., Prevot, A. S. H., and Guo, S.: Secondary organic aerosol formation in China from urban-lifestyle sources: Vehicle exhaust and cooking emission, Sci. Total Environ., 857, 159340, https://doi.org/10.1016/j.scitotenv.2022.159340, 2022.
Zhao, Y., Tkacik, D. S., May, A. A., Donahue, N. M., and Robinson, A. L.: Mobile sources are still an important source of secondary organic aerosol and fine particulate matter in the los angeles region, Environ. Sci. Technol., 56, 15328-15336, https://doi.org/10.1021/acs.est.2c03317, 2022a.
Zhao, Y., Xi, M., Zhang, Q., Dong, Z., Ma, M., Zhou, K., Xu, W., Xing, J., Zheng, B., Wen, Z., Liu, X., Nielsen, C. P., Liu, Y., Pan, Y., and Zhang, L.: Decline in bulk deposition of air pollutants in China lags behind reductions in emissions, Nat. Geosci., 15, 190-195, https://doi.org/10.1038/s41561-022-00899-1, 2022b.
Zheng, L., Chen, W., Jia, S., Wu, L., Zhong, B., Liao, W., Chang, M., Wang, W., and Wang, X.: Temporal and spatial patterns of nitrogen wet deposition in different weather types in the Pearl River Delta (PRD), China, Sci. Total Environ., 740, 139936, https://doi.org/10.1016/j.scitotenv.2020.139936, 2020.
Zhu, J., He, N., Wang, Q., Yuan, G., Wen, D., Yu, G., and Jia, Y.: The composition, spatial patterns, and influencing factors of atmospheric wet nitrogen deposition in Chinese terrestrial ecosystems, Sci. Total Environ., 511, 777-785, https://doi.org/10.1016/j.scitotenv.2014.12.038, 2015.
Zong, Z., Shi, X., Sun, Z., Tian, C., Li, J., Fang, Y., Gao, H., and Zhang, G.: Nitrogen isotopic composition of NOx from residential biomass burning and coal combustion in North China, Environ. Pollut., 304, 119238, https://doi.org/10.1016/j.envpol.2022.119238, 2022.
Zong, Z., Tan, Y., Wang, X., Tian, C., Li, J., Fang, Y., Chen, Y., Cui, S., and Zhang, G.: Dual-modelling-based source apportionment of NOx in five Chinese megacities: providing the isotopic footprint from 2013 to 2014,

761 Environ. Int., 137, 105592, https://doi.org/10.1016/j.envint.2020.105592, 2020.
762 Zong, Z., Wang, X., Tian, C., Chen, Y., Fang, Y., Zhang, F., Li, C., Sun, J., Li, J., and Zhang, G.: First assessment
763 of NOx sources at a regional background site in North China using isotopic analysis linked with modeling,
764 Environ. Sci. Technol., 51, 5923-5931, https://doi.org/10.1021/acs.est.6b06316, 2017.
765

Supplement of

High contribution of anthropogenic combustion sources to atmospheric inorganic reactive nitrogen in South China evidenced by isotopes

Tingting Li[1,2,4], Jun Li[*1,2], Zeyu Sun[3,4], Hongxing Jiang[1], Chongguo Tian[3], Gan Zhang[1,2]

[1]State Key Laboratory of Organic Geochemistry and Guangdong province Key Laboratory of Environmental Protection and Resources Utilization, Guangdong-Hong Kong-Macao Joint Laboratory for Environmental Pollution and Control, Guangzhou Institute of Geochemistry, Chinese Academy of Sciences, Guangzhou, 510640, China
[2]CAS Center for Excellence in Deep Earth Science, Guangzhou 510640, P. R. China
[3]Yantai Institute of Coastal Zone Research, Chinese Academy of Sciences, Yantai 264003, P. R. China
[4]University of Chinese Academy of Sciences, Beijing 100049, P. R. China
**Correspondence to*: Jun Li (junli@gig.ac.cn)

Contents:

Text S1 Chemical components analysis

OC/EC: OC and EC contents were analyzed by thermal-optical carbon analyzer (Sunset Laboratory Inc). One punch of 1.5 cm^2 filter samples was cut and put into the instrument. Blank samples were measured by the same methods. Quality control standards (sucrose solutions) were dropped onto quartz membranes to dry and then the carbon content was tested in the same way to ensure that the instrument was stable before measurement and in the testing process.

Water-soluble ions: Na^+, K^+, Mg^{2+}, Ca^{2+}, NH_4^+, Cl^-, SO_4^{2-}, and NO_3^- were measured by ion chromatography. The blank samples were also analyzed following the same procedure for samples. Reagent blanks (ultrapure water) and quality control standards were measured every 10 samples to detect contamination and drift.

Isotopic analysis: The $\delta^{15}N\text{-}NO_3^-$ and $\delta^{18}O\text{-}NO_3^-$ values (‰) were corrected by multi-point correction (r^2=0.999) based on international standards (IAEA-NO3, USGS32, USGS34, and USGS35) and $\delta^{15}N\text{-}NH_4^+$ was corrected by international standards (IAEA-N1, USGS25, and USGS26) (Sun et al., 2021; Zong et al., 2017).

Radioactive isotope analysis: ^{210}Pb and ^{7}Be were analyzed at Shenzhen University using high-purity γ spectrometer equipped with an HPGe detector (Jiang et al., 2021; Liu et al., 2020). ^{210}Pb in the atmosphere mainly comes from terrestrial sources and is effective indicator of the aerosols transport from the continental surface. The $f(^{7}Be, ^{210}Pb)$ index is powerful to reveal the influence of atmospheric dynamic transport on variations in aerosol pollutants, and expressed as following equation (Jiang et al., 2021). Generally, the relatively high values of $f(^{7}Be, ^{210}Pb)$ index represented that the aerosol pollutants were influenced by ~~long~~ long-range transport from the upper air.

$$f(^{7}Be,^{210}Pb) = \frac{[^{7}Be]}{[^{7}Be]+n[^{210}Pb]} \quad (S1)$$

where $[^{7}Be]$ and $[^{210}Pb]$ are activity concentrations of ^{7}Be and ^{210}Pb, respectively, n is estimated as the ratio of the standard deviation of $[^{7}Be]$ to $[^{210}Pb]$.

Trace gas: concentrations of trace gases (NO, NO_2, SO_2, O_3, and CO) were acquired from online equipment. The online equipment included a gas filter analyzer (Thermo Scientific, Model 48i) to measure CO, a pulse fluorescence analyzer (Thermo

Scientific, Model 43iTLE) to measure SO_2 and O_3, and a chemiluminescence apparatus (Thermo Scientific, Model 42iTL) to measure NO and NO_2.

Meteorological parameters: Temperature, relative humidity, wind speed, and atmospheric pressure were also acquired by a portable weather analyzer (WXT520, Vaisala, Finland). Trace gas concentrations and meteorological parameters were hourly data. In this study, average data of 24 hours through a sampling period were used.

Text S2 Sources of atmospheric NH_3 and NOx in Guangzhou, NO_3^- formation pathways in Guangzhou

Atmospheric NH_3 sources. There are two major groups of atmospheric NH_3 emission sources(Chen et al., 2022b). One is NH_3 volatilization from NH_4^+-containing substrates (mainly fertilized and natural soils, livestock, human wastes, and natural and N-polluted water). Although Guangzhou is an urban site, the emission inventory results showed a high contribution of nitrogen fertilizers application and livestock to atmospheric NH_3 (Zheng et al., 2012), which may be influenced by agricultural activities around Guangzhou. Human waste is also an important contributor to NH_3 in cities, as suggested by a study in Shanghai(Chang et al., 2015). Guangzhou is one of China's megacities with a dense population, so the contribution of human waste to atmospheric NH_3 in Guangzhou cannot be ignored. Therefore, nitrogen fertilizers application, livestock, and human waste were considered as sources of volatilization NH_3 in this study. In addition, the other group is NH_3 associated with combustion sources (such as coal burning, vehicles, and biomass burning). The contribution of biomass burning and coal combustion to NH_3 was very high (about 76.3%) in developing countries, as suggested by the global high-resolution emissions inventory (Meng et al., 2017). NH_3 in Chinese cities was indeed influenced by coal and biomass combustion evidenced by isotopes(Xiao et al., 2020; Liu et al., 2018; Pan et al., 2018). Selective catalytic reduction technology equipped with vehicles and industrial boiler is also an important source of NH_3(Meng et al., 2017). With the rapid increase in vehicle ownership, vehicle emission has a significant impact on urban NH_3, which was confirmed by tunnel tests in Guangzhou (Liu et al., 2014). Therefore, biomass burning,

coal combustion, and vehicles were considered as sources of combustion NH_3 in this study.

Atmospheric NOx sources. We considered coal combustion, mobile traffic sources, biomass burning, and soil microbial activity as dominant atmospheric NOx sources. Based on bottom-up emission inventory, power plant, industry, residential use, and transportation were the traditional NOx emission sources in cities in China, including Guangzhou (Liu et al., 2017a). According to the type of fuel combustion, traditional sources of NOx could be roughly divided into coal combustion (power plant, industry, and residential use) and mobile sources (transportation including vehicle exhaust and ship emission). Furthermore, recent studies show that biomass burning is an essential source of NOx based on emission factor study (Mehmood et al., 2017) and isotopic evidence (Zong et al., 2020). Microbial process emission is another important source of NOx, in which nitrification or denitrification microbial bacteria widely distributed in soils consume accumulated nitrogen and release NO as a byproduct(Hall and Matson, 1996; Jaeglé et al., 2004). The cultivated land with extensive use of nitrogen fertilizer in the suburbs around Guangzhou is also an important source of NOx, which is named as microbial process in this study. δ^{15}N-NOx values differed significantly among these four sources, which allows us to differentiate their relative contributions to the mixture of atmospheric. We did not consider NO_3^- from lightning because it accounts for less than 5% of global terrestrial NOx emissions(Song et al., 2021; Qu et al., 2020; Pickering et al., 2016).

NO_3^- formation pathways. There are several major formation pathways of NO_3^-.

P1 (NO_2+·OH), NO_2 is oxidized by ·OH to form HNO_3, then reacts with alkaline substances (such as NH_3) to form NO_3^-.

P2 (N_2O_5), NO_2 is oxidized by O_3 to form ·NO_3, ·NO_3 reacts with NO_2 to form N_2O_5, then the hydrolysis of N_2O_5 on aerosol surfaces produces NO_3^-.

P3 (·NO_3+org), the NO_2 is oxidized by O_3 to form ·NO_3, then the ·NO_3 reacts with organic, such as dimethyl sulfide (DMS) or hydrocarbons (HC) to form HNO_3, and then NO_3^-.

P4(·NO_3+·HO_2), NO_2 is oxidized by O_3 to form ·NO_3, ·NO_3 reacts with ·HO_2 to

form HNO_3.

The P1 (·OH) and P2 (N_2O_5) pathways are dominant formation pathways. Song reported that ·OH and N_2O_5 pathways contributed 43% and 32% to NO_3^-, respectively, by isotope tracing (Song et al., 2021). Based on isotopic estimates, the contribution of ·NO3+org to NO_3^- was relatively high, e.g., about 16% in Beijing(Song et al., 2021). However, the proportion of $\cdot NO_3$+org estimated by the Community Multiscale Air Quality (CAMQ) model was very low in the YRD(Sun et al., 2022) and PRD(Qu et al., 2021), especially in Guangzhou (central PRD) where it is only 4%(Qu et al., 2021). The ·OH and N_2O_5 were the dominant pathways and contributed 94% to NO_3^- in Guangzhou (Qu et al., 2021). We speculate that the different contribution of $\cdot NO_3$+org pathway between Guangzhou and Beijing may be caused by the difference in atmospheric oxidation. The ozone pollution is serious in Guangzhou due to a unique synoptic system including the surface high-pressure system, hurricane movement, and sea–land breeze(Tan et al., 2019). And the atmospheric ·OH reactivity in Guangzhou was higher than in several cities, including Beijing (Tan et al., 2019). Take DMS as an example, the main oxidant of DMS is ·OH (Andreae and Crutzen, 1997). However, in the cold season or remote regions, the $\cdot NO_3$ radical can also play an important role in reaction with DMS (addition reaction and hydrogen abstraction) (Andreae and Crutzen, 1997; Yin et al., 1990). The high reactivity of ·OH may reduce the contribution of $\cdot NO_3$ to DMS in Guangzhou due to the competition between ·OH and $\cdot NO_3$ to react with DMS. Therefore, the contribution of $\cdot NO_3$+org to NO_3^- was relatively low. In addition, the $\delta^{18}O$ of NO_3^- formed by the N_2O_5 and $\cdot NO_3$+org pathway is similar(Walters and Michalski, 2016). The introduction of the $\cdot NO_3$+org pathway would greatly increase the uncertainty of the contribution of N_2O_5 pathways. While the $\delta^{18}O$ of NO_3^- formed by the ·OH and N_2O_5 pathway differ significantly, which allows to differentiate their relative contributions to NO_3^-. Therefore, we considered only the ·OH and N_2O_5 pathways in this study.

Specifically, the ·OH and N_2O_5 pathways are expressed by R1-R8. Once emitted into the atmosphere, NOx is oxidized to HNO_3 or NO_3^- via the following chemical pathways (R1-R8) (Fang et al., 2011). In summary, NOx oxygen atoms are rapidly

exchanged with O_3 in the NO/NO_2 cycle (R1-R3); ·OH radicals result in the oxidation of NO_2 to HNO_3 (R4; the ·OH pathway); NO_2 is oxidized by O_3 to produce ·NO_3 (R5), which subsequently combines with NO_2 to form N_2O_5 (R6), and then undergoes hydrolysis to form HNO_3 (R7), referred to as the O_3 pathway; and the generated HNO_3 combines with alkali to form NO_3^- (R8). Overall, the ·OH and O_3 pathways are the two fundamental oxidation pathways for NOx, generally exhibiting noticeable diurnal and seasonal variation(Elliott et al., 2007). Previous research has found that the ·OH pathway is more prevalent during the daytime and in summer when the relative concentration of ·OH is higher. Conversely, the O_3 pathway is more dominant overnight and in winter, because N_2O_5 is thermally unstable(Hastings et al., 2003; Xiao et al., 2015). The O_3 in the troposphere has a higher $\delta^{18}O$ value, while $\delta^{18}O$-OH and $\delta^{18}O$-H_2O is lower. The $\delta^{18}O$-HNO_3 formed by the ·OH pathway is contributed by 2/3 O_3 and 1/3 ·OH (R4), while in the N_2O_5 hydrolysis pathway after oxidation by O_3, the $\delta^{18}O$-HNO_3 is contributed by 5/6 O_3 and 1/6 H_2O (R5-R7). Therefore, the $\delta^{18}O$-NO_3^- formed through the ·OH pathway is lower than the N_2O_5 pathway.

$$NO + O_3 \rightarrow NO_2 + O_2 \quad (R1)$$

$$NO_2 + hv \rightarrow NO + O \quad (R2)$$

$$O + O_2 \rightarrow O_3 \quad (R3)$$

$$NO_2 + \cdot OH \rightarrow HNO_3 \quad (R4)$$

$$NO_2 + O_3 \rightarrow NO_3 + O_2 \quad (R5)$$

$$NO_2 + NO_3 \rightarrow N_2O_5 \quad (R6)$$

$$N_2O_5 + H_2O \rightarrow 2HNO_3 \quad (R7)$$

$$HNO_3 + Alkali \rightarrow NO_3^- \quad (R8)$$

Text S3 The estimation of $\delta^{15}N$-NH_4^+ from sugarcane leaf burning

The $\delta^{15}N$ in sugarcane leaf is 38‰ (Martinellia et al., 2002), which may consist of N-NO_X and N-NH_3. The $\delta^{15}N$-NOx from biomass burning is 1.04‰(Zong et al., 2017). According to the assumption of different proportions (from 5% to 95%) of N-NO_X and N-NH_3 from sugarcane leaf, shown in **Table S3~~3~~2**. The mean value among the proportion (from 5% to 95%) of N-NH_4^+ in sugarcane leaf was 37.48‰. In addition, the $\delta^{15}N$ of

particulate matters from biomass burning was 6.6‰ higher than that of biomass (Martinellia et al., 2002). Therefore, $\delta^{15}N\text{-}NH_4^+$ from sugarcane leaf burning may be 44.08‰.

Figure S1-Figure S6

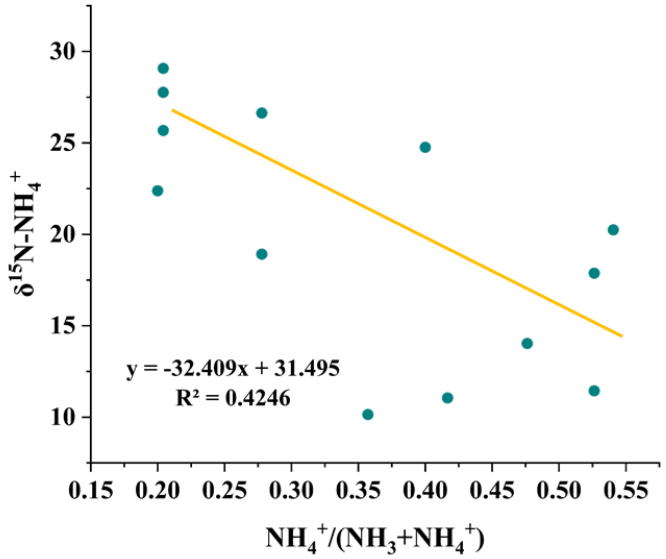

Figure ~~S2~~S1. Linear fitting of $NH_4^+/(NH_3+NH_4^+)$ with δ^{15}N-NH_4^+.

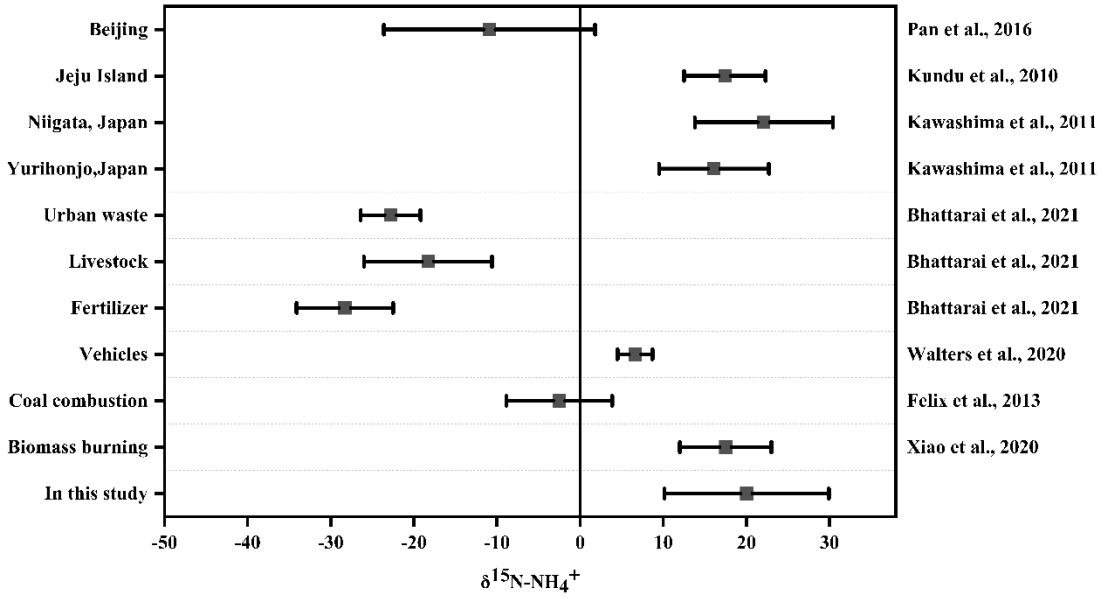

Figure ~~S1~~2. Ranges of δ^{15}N-NH_4^+ from different sites(Pan et al., 2016; Kundu et al., 2010; Kawashima and Kurahashi, 2011) and different emission sources(Felix et al., 2013; Bhattarai et al., 2021; Chang et al., 2016; Xiao et al., 2020).

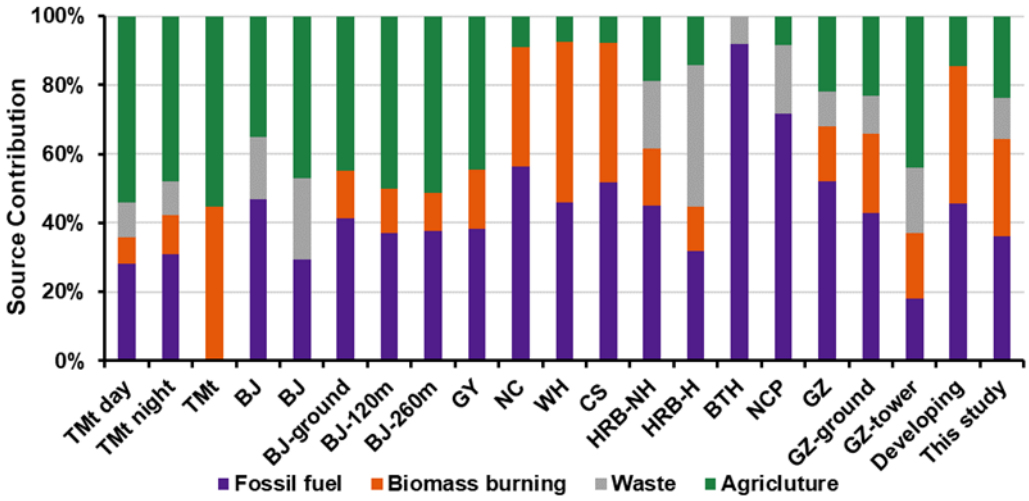

Figure S3. The comparison of sources apportionment results of atmospheric NH_3 and NH_4^+ in different sites in China. Background site in Tai mountain[TMt] (Wu et al., 2021; Chang et al., 2019), urban sites in North China (Beijing [BJ] (Pan et al., 2020; Chang et al., 2016), vertical profile observation in Beijing (ground, 120m height, and 260m height [BJ-ground, BJ-120m, and BJ-260m] (Wu et al., 2019), Jingjinji region [BTH] (Zhang et al., 2020), and North China plain [NCP]) (Xiang et al., 2022), East North China (Harbin heating period and non-heating period [HRB-H and HRB-NH]) (Sun et al., 2021), Central China (Wuhan [WH] and Changsha [CS]) (Xiao et al., 2020), East China (Nangchang [NC]) (Xiao et al., 2020), Southwest China (Guiyang [GY], source in precipitation) (Liu et al., 2017b), and South China (Guangzhou[GZ]) (Liu et al., 2018), vertical profile observation in Guangzhou(ground and Guangzhou tower [GZ-ground and GZ-tower])(Chen et al., 2022a). Source of NH_3 were estimated by inventory methods in developing country[developing] (Meng et al., 2017).

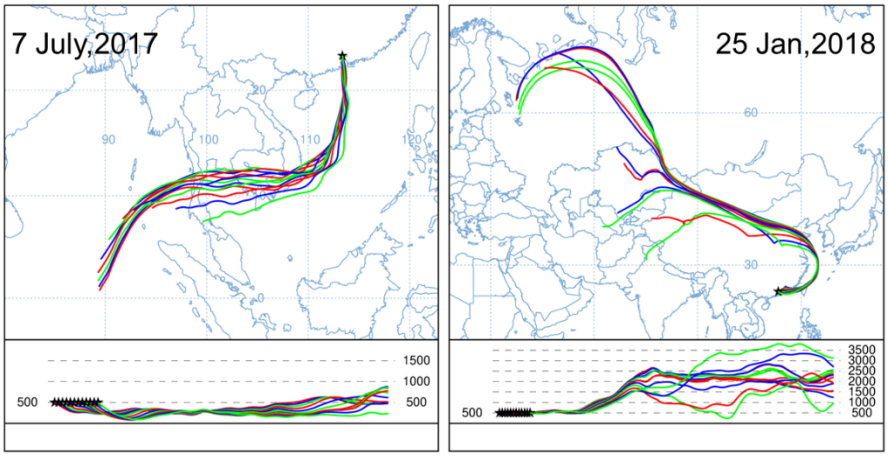

195

196 **Figure S4.** The air mass backward trajectory to receptor site on 7 July,2017 and 25

197 Jan,2018.

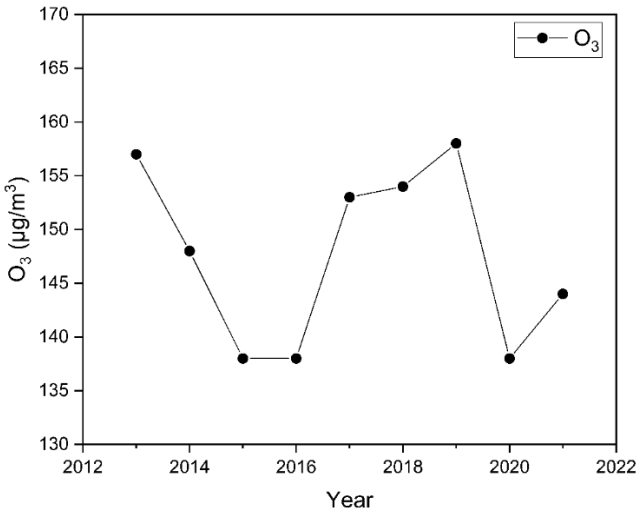

198

199 **Figure S5.** The temporal variation of O_3 concentration in PRD from 2013 to 2021.

200

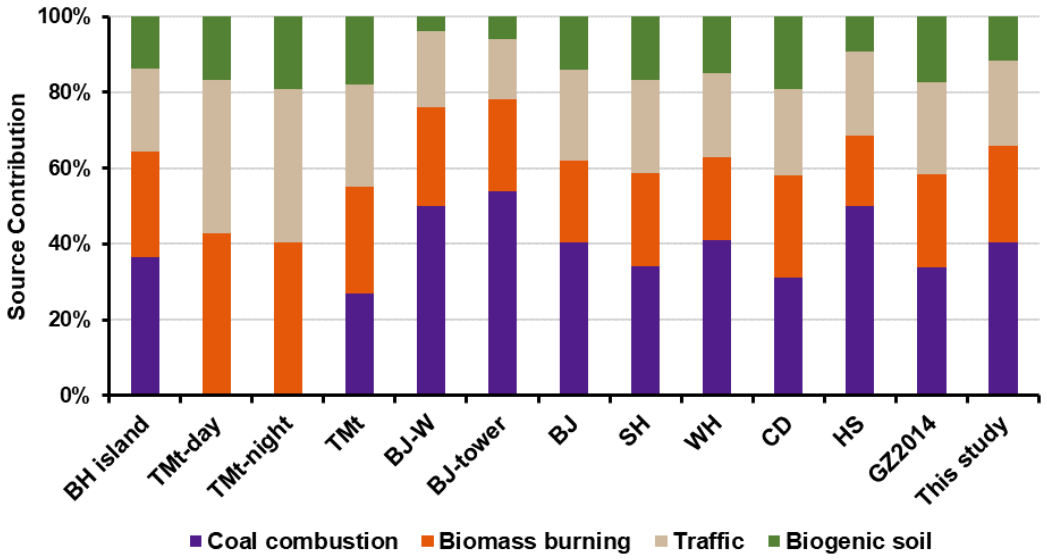

Figure S6. The comparison of sources apportionment results of atmospheric NOx and NO_3^- in different sites in China. Background in ~~Tuoji~~ Beihuangcheng island [~~TJ~~ BH island](Zong et al., 2017) and Tai mountain [TMt] (Wu et al., 2021), urban sites in North China (Beijing [BJ] (Zong et al., 2020), Beijing winter [BJ-W] (Fan et al., 2020), and vertical profile observation in Beijing [BJ-tower](Fan et al., 2022)), Central China (Wuhan [WH]) (Zong et al., 2020), East China (Shanghai [SH]) (Zong et al., 2020), Southwest China (Chengdu [CD]), and South China (Guangzhou [GZ2014] and Heshan [HS])(Zong et al., 2020; Su et al., 2020).

Table S1-Table S2

Table S1. Test constants of A, B, C, and D over the settled temperature range of 150−450K(Zong et al., 2017; Walters and Michalski, 2016; Walters et al., 2016; Walters and Michalski, 2015).

$^{m}\alpha_{X/Y}$	A	B	C	D
$^{15}NO_2/NO$	3.8834	-7.7299	6.0101	-0.17928
$^{15}N_2O_5/NO_2$	0.69398	-1.9859	2.3876	0.16308
$^{18}NO/NO_2$	-0.04129	1.1605	-1.8829	0.74723
$^{18}H_2O/OH$	2.1137	-3.8026	2.5653	0.59410

Table S~~3~~2. The estimation of δ^{15}N-NH_3 in sugarcane leaf.

N-NOx in sugarcane leaf (%)	5	25	50	75	95
δ^{15}N in sugarcane leaf (‰)	38	38	38	38	38
δ^{15}N-NOx (‰)	1.04	1.04	1.04	1.04	1.04
Caculated results δ^{15}N-NH_3 (‰)	37.95	37.74	37.48	37.22	37.01

References:

Andreae, M. O. and Crutzen, P. J.: Atmospheric aerosols: biogeochemical sources and role in atmospheric chemistry, Science, 276, 1052-1058, https://doi.org/10.1126/science.276.5315.1052, 1997.

Bhattarai, N., Wang, S., Pan, Y., Xu, Q., Zhang, Y., Chang, Y., and Fang, Y.: δ^{15}N-stable isotope analysis of NHx : An overview on analytical measurements, source sampling and its source apportionment, Front. Environ. Sci. Eng., 15, 126, https://doi.org/10.1007/s11783-021-1414-6, 2021.

Chang, Y., Deng, C., Dore, A. J., and Zhuang, G.: Human Excreta as a Stable and Important Source of Atmospheric Ammonia in the Megacity of Shanghai, PLoS One, 10, e0144661, https://doi.org/10.1371/journal.pone.0144661, 2015.

Chang, Y., Liu, X., Deng, C., Dore, A. J., and Zhuang, G.: Source apportionment of atmospheric ammonia before, during, and after the 2014 APEC summit in Beijing using stable nitrogen isotope signatures, Atmos. Chem. Phys., 16, 11635-11647, https://doi.org/10.5194/acp-16-11635-2016, 2016.

Chang, Y., Zhang, Y.-L., Li, J., Tian, C., Song, L., Zhai, X., Zhang, W., Huang, T., Lin, Y.-C., Zhu, C., Fang, Y., Lehmann, M. F., and Chen, J.: Isotopic constraints on the atmospheric sources and formation of nitrogenous species in clouds influenced by biomass burning, Atmos. Chem. Phys., 19, 12221–12234, https://doi.org/10.5194/acp-19-12221-2019, 2019.

Chen, Z., Pei, C., Liu, J., Zhang, X., Ding, P., Dang, L., Zong, Z., Jiang, F., Wu, L., Sun, X., Zhou, S., Zhang, Y., Zhang, Z., Zheng, J., Tian, C., Li, J., and Zhang, G.: Non-agricultural source dominates the ammonium aerosol in the largest city of South China based on the vertical δ^{15}N measurements,

Sci. Total Environ., 848, 157750, https://doi.org/10.1016/j.scitotenv.2022.157750, 2022a.

Chen, Z. L., Song, W., Hu, C. C., Liu, X. J., Chen, G. Y., Walters, W. W., Michalski, G., Liu, C. Q., Fowler, D., and Liu, X. Y.: Significant contributions of combustion-related sources to ammonia emissions, Nat. Commun., 13, 7710, https://doi.org/10.1038/s41467-022-35381-4, 2022b.

Elliott, E. M., Kendall, C., Wankel, S. D., Burns, D. A., Boyer, E. W., Harlin, K., Bain, D. J., and Butler, T. J.: Nitrogen isotopes as indicators of NOx source contributions to atmospheric nitrate deposition across the midwestern and Northeastern United States, Environ. Sci. Technol., 41, 7661-7667, https://doi.org/10.1021/es070898t, 2007.

Fan, M.-Y., Zhang, Y.-L., Hong, Y., Lin, Y.-C., Zhao, Z.-Y., Cao, F., Sun, Y., Guo, H., and Fu, P.: Vertical differences of nitrate sources in urban boundary layer based on tower measurements, Environ. Sci. Technol. Lett., 2c00600, https://doi.org/10.1021/acs.estlett.2c00600, 2022.

Fan, M. Y., Zhang, Y. L., Lin, Y. C., Cao, F., Zhao, Z. Y., Sun, Y., Qiu, Y., Fu, P., and Wang, Y.: Changes of emission sources to nitrate aerosols in Beijing after the clean air actions: evidence from dual isotope compositions, J. Geophys. Res.: Atmos., 125, 031998, https://doi.org/10.1029/2019jd031998, 2020.

Fang, Y. T., Koba, K., Wang, X. M., Wen, D. Z., Li, J., Takebayashi, Y., Liu, X. Y., and Yoh, M.: Anthropogenic imprints on nitrogen and oxygen isotopic composition of precipitation nitrate in a nitrogen-polluted city in southern China, Atmos. Chem. Phys., 11, 1313-1325, https://doi.org/10.5194/acp-11-1313-2011, 2011.

Felix, J. D., Elliott, E. M., Gish, T. J., McConnell, L. L., and Shaw, S. L.: Characterizing the isotopic composition of atmospheric ammonia emission sources using passive samplers and a combined oxidation-bacterial denitrifier approach, Rapid Commun. Mass Spectrom., 27, 2239-2246, https://doi.org/10.1002/rcm.6679, 2013.

Hall, S. J. and Matson, P. A.: NOx emissions from soil: implications for air quality modeling in agricultural regions, Annu. Rev. Energy Environ., 21, 311-346, https://doi.org/10.1146/annurev.energy.21.1.311, 1996.

Hastings, M. G., Sigman, D. M., and Lipschultz, F.: Isotopic evidence for source changes of nitrate in rain at Bermuda, J. Geophys. Res.: Atmos., 108, 1-12, https://doi.org/10.1029/2003jd003789, 2003.

Jaeglé, L., Martin, R. V., Chance, K., Steinberger, L., Kurosu, T. P., Jacob, D. J., Modi, A. I., Yoboué, V., Sigha-Nkamdjou, L., and Galy-Lacaux, C.: Satellite mapping of rain-induced nitric oxide emissions from soils, J. Geophys. Res.: Atmos., 109, D21310, https://doi.org/10.1029/2004jd004787, 2004.

Jiang, H., Li, J., Sun, R., Liu, G., Tian, C., Tang, J., Cheng, Z., Zhu, S., Zhong, G., Ding, X., and Zhang, G.: Determining the sources and transport of brown carbon using radionuclide tracers and modeling, J. Geophys. Res.: Atmos., 126, e2021JD034616, https://doi.org/10.1029/2021jd034616, 2021.

Kawashima, H. and Kurahashi, T.: Inorganic ion and nitrogen isotopic compositions of atmospheric aerosols at Yurihonjo, Japan: implications for nitrogen sources, Atmos. Environ., 45, 6309-6316, https://doi.org/10.1016/j.atmosenv.2011.08.057, 2011.

Kundu, S., Kawamura, K., and Lee, M.: Seasonal variation of the concentrations of nitrogenous species and their nitrogen isotopic ratios in aerosols at Gosan, Jeju Island: Implications for atmospheric processing and source changes of aerosols, J. Geophys. Res. , 115, https://doi.org/10.1029/2009jd013323, 2010.

Liu, F., Beirle, S., Zhang, Q., van der, A. R., Zheng, B., Tong, D., and He, K.: NOx emission trends over Chinese cities estimated from OMI observations during 2005 to 2015, Atmos. Chem. Phys., 17, 9261-9275, https://doi.org/10.5194/acp-17-9261-2017, 2017a.

Liu, G., Wu, J., Li, Y., Su, L., and Ding, M.: Temporal variations of ^{7}Be and ^{210}Pb activity concentrations in the atmosphere and aerosol deposition velocity in Shenzhen, South China, Aerosol Air Qual. Res., 20, 1607–1617, https://doi.org/10.4209/aaqr.2019.11.0560, 2020.

Liu, J., Ding, P., Zong, Z., Li, J., Tian, C., Chen, W., Chang, M., Salazar, G., Shen, C., Cheng, Z., Chen, Y., Wang, X., Szidat, S., and Zhang, G.: Evidence of rural and suburban sources of urban haze formation in China: a case study from the Pearl River Delta region, J. Geophys. Res.: Atmos., 123, 4712-4726, https://doi.org/10.1029/2017jd027952, 2018.

Liu, T., Wang, X., Wang, B., Ding, X., Deng, W., Lü, S., and Zhang, Y.: Emission factor of ammonia (NH_3) from on-road vehicles in China: tunnel tests in urban Guangzhou, Environ. Res. Lett., 9, 064027, https://doi.org/10.1088/1748-9326/9/6/064027, 2014.

Liu, X. Y., Xiao, H. W., Xiao, H. Y., Song, W., Sun, X. C., Zheng, X. D., Liu, C. Q., and Koba, K.: Stable isotope analyses of precipitation nitrogen sources in Guiyang, southwestern China, Environ. Pollut., 230, 486-494, https://doi.org/10.1016/j.envpol.2017.06.010, 2017b.

Martinellia, L. A., Camargoa, P. B., Laraa, L. B. L. S., Victoriaa, R. L., and Artaxo, P.: Stable carbon and nitrogen isotopic composition of bulk aerosol particles in a C4 plant landscape of southeast Brazil, Atmos. Environ., 36, 2427–2432, https://doi.org/10.1016/S1352-2310(01)00454-X, 2002.

Mehmood, K., Chang, S., Yu, S., Wang, L., Li, P., Li, Z., Liu, W., Rosenfeld, D., and Seinfeld, J. H.: Spatial and temporal distributions of air pollutant emissions from open crop straw and biomass burnings in China from 2002 to 2016, Environ. Chem. Lett., 16, 301-309, https://doi.org/10.1007/s10311-017-0675-6, 2017.

Meng, W., Zhong, Q., Yun, X., Zhu, X., Huang, T., Shen, H., Chen, Y., Chen, H., Zhou, F., Liu, J., Wang, X., Zeng, E. Y., and Tao, S.: Improvement of a global high-resolution ammonia emission inventory for combustion and industrial sources with new data from the residential and transportation sectors, Environ. Sci. Technol., 51, 2821-2829, https://doi.org/10.1021/acs.est.6b03694, 2017.

Pan, Y., Tian, S., Liu, D., Fang, Y., Zhu, X., Zhang, Q., Zheng, B., Michalski, G., and Wang, Y.: Fossil fuel combustion-related emissions dominate atmospheric ammonia sources during severe haze episodes: evidence from ^{15}N-stable isotope in size-resolved aerosol ammonium, Environ. Sci. Technol., 50, 8049-8056, https://doi.org/10.1021/acs.est.6b00634, 2016.

Pan, Y., Tian, S., Liu, D., Fang, Y., Zhu, X., Gao, M., Wentworth, G. R., Michalski, G., Huang, X., and Wang, Y.: Source Apportionment of Aerosol Ammonium in an Ammonia-Rich Atmosphere: An Isotopic Study of Summer Clean and Hazy Days in Urban Beijing, J. Geophys. Res.: Atmos., 123, 5681-5689, https://doi.org/10.1029/2017jd028095, 2018.

Pan, Y., Gu, M., He, Y., Wu, D., Liu, C., Song, L., Tian, S., Lü, X., Sun, Y., Song, T., Walters, W. W., Liu, X., Martin, N. A., Zhang, Q., Fang, Y., Ferracci, V., and Wang, Y.: Revisiting the concentration observations and source apportionment of atmospheric ammonia, Adv. Atmos. Sci., 37, 933-938, https://doi.org/10.1007/s00376-020-2111-2, 2020.

Pickering, K. E., Bucsela, E., Allen, D., Ring, A., Holzworth, R., and Krotkov, N.: Estimates of lightning NOx production based on OMI NO_2 observations over the Gulf of Mexico, J. Geophys. Res.: Atmos., 121, 8668-8691, https://doi.org/10.1002/2015jd024179, 2016.

Qu, K., Wang, X., Xiao, T., Shen, J., Lin, T., Chen, D., He, L. Y., Huang, X. F., Zeng, L., Lu, K., Ou, Y., and Zhang, Y.: Cross-regional transport of $PM_{2.5}$ nitrate in the Pearl River Delta, China: Contributions and mechanisms, Sci. Total Environ., 753, 142439, https://doi.org/10.1016/j.scitotenv.2020.142439, 2021.

Qu, Z., Henze, D. K., Cooper, O. R., and Neu, J. L.: Impacts of global NOx inversions on NO_2 and ozone

simulations, Atmos. Chem. Phys., 20, 13109-13130, https://doi.org/10.5194/acp-20-13109-2020, 2020.

Song, W., Liu, X. Y., and Liu, C. Q.: New Constraints on Isotopic Effects and Major Sources of Nitrate in Atmospheric Particulates by Combining $\delta^{15}N$ and $\Delta^{17}O$ Signatures, J. Geophys. Res.: Atmos., 126, https://doi.org/10.1029/2020jd034168, 2021.

Su, T., Li, J., Tian, C., Zong, Z., Chen, D., and Zhang, G.: Source and formation of fine particulate nitrate in South China: Constrained by isotopic modeling and online trace gas analysis, Atmos. Environ., 231, https://doi.org/10.1016/j.atmosenv.2020.117563, 2020.

Sun, J., Qin, M., Xie, X., Fu, W., Qin, Y., Sheng, L., Li, L., Li, J., Sulaymon, I. D., Jiang, L., Huang, L., Yu, X., and Hu, J.: Seasonal modeling analysis of nitrate formation pathways in Yangtze River Delta region, China, Atmos. Chem. Phys., 22, 12629-12646, https://doi.org/10.5194/acp-22-12629-2022, 2022.

Sun, X., Zong, Z., Li, Q., Shi, X., Wang, K., Lu, L., Li, B., Qi, H., and Tian, C.: Assessing the emission sources and reduction potential of atmospheric ammonia at an urban site in Northeast China, Environ. Res., 198, 111230, https://doi.org/10.1016/j.envres.2021.111230, 2021.

Tan, Z., Lu, K., Jiang, M., Su, R., Wang, H., Lou, S., Fu, Q., Zhai, C., Tan, Q., Yue, D., Chen, D., Wang, Z., Xie, S., Zeng, L., and Zhang, Y.: Daytime atmospheric oxidation capacity in four Chinese megacities during the photochemically polluted season: a case study based on box model simulation, Atmos. Chem. Phys., 19, 3493–3513, https://doi.org/10.5194/acp-19-3493-2019, 2019.

Walters, W. W. and Michalski, G.: Theoretical calculation of nitrogen isotope equilibrium exchange fractionation factors for various NOy molecules, Geochim. Cosmochim. Ac., 164, 284-297, https://doi.org/10.1016/j.gca.2015.05.029, 2015.

Walters, W. W. and Michalski, G.: Theoretical calculation of oxygen equilibrium isotope fractionation factors involving various NOy molecules, OH, and H_2O and its implications for isotope variations in atmospheric nitrate, Geochim. Cosmochim. Ac., 191, 89–101 https://doi.org/10.1016/j.gca.2016.06.039, 2016.

Walters, W. W., Simonini, D. S., and Michalski, G.: Nitrogen isotope exchange between NO and NO_2 and its implications for $\delta^{15}N$ variations in tropospheric NOx and atmospheric nitrate, Geophys. Res. Lett., 43, 440-448, https://doi.org/10.1002/2015gl066438, 2016.

Wu, L., Yue, S., Shi, Z., Hu, W., Chen, J., Ren, H., Deng, J., Ren, L., Fang, Y., Li, W., Harrison, R. M., and Fu, P.: Source forensics of inorganic and organic nitrogen using δ15N for tropospheric aerosols over Mt. Tai, npj Clim. Atmos. Sci., 8, https://doi.org/10.1038/s41612-021-00163-0, 2021.

Wu, L., Ren, H., Wang, P., Chen, J., Fang, Y., Hu, W., Ren, L., Deng, J., Song, Y., Li, J., Sun, Y., Wang, Z., Liu, C.-Q., Ying, Q., and Fu, P.: Aerosol ammonium in the urban boundary layer in Beijing: insights from nitrogen isotope ratios and simulations in summer 2015, Environ. Sci. Technol. Lett., 6, 389-395, https://doi.org/10.1021/acs.estlett.9b00328, 2019.

Xiang, Y.-K., Dao, X., Gao, M., Lin, Y.-C., Cao, F., Yang, X.-Y., and Zhang, Y.-L.: Nitrogen isotope characteristics and source apportionment of atmospheric ammonium in urban cities during a haze event in Northern China Plain, Atmos. Environ., 269, 118800, https://doi.org/10.1016/j.atmosenv.2021.118800, 2022.

Xiao, H.-W., Xie, L.-H., Long, A.-M., Ye, F., Pan, Y.-P., Li, D.-N., Long, Z.-H., Chen, L., Xiao, H.-Y., and Liu, C.-Q.: Use of isotopic compositions of nitrate in TSP to identify sources and chemistry in South China Sea, Atmos. Environ., 109, 70-78, https://doi.org/10.1016/j.atmosenv.2015.03.006, 2015.

Xiao, H. W., Wu, J. F., Luo, L., Liu, C., Xie, Y. J., and Xiao, H. Y.: Enhanced biomass burning as a source of aerosol ammonium over cities in central China in autumn, Environ. Pollut., 266, 115278, https://doi.org/10.1016/j.envpol.2020.115278, 2020.

Yin, F., Grosjean, D., and Seinfeld, J. H.: Photooxidation of Dimethyl Sulfide and Dimethyl Disulfide. I: Mechanism Development, J. Atmos. Chem., 11, 309-364, 1990.

Zhang, Z., Zeng, Y., Zheng, N., Luo, L., Xiao, H., and Xiao, H.: Fossil fuel-related emissions were the major source of NH_3 pollution in urban cities of northern China in the autumn of 2017, Environ. Pollut., 256, 113428, https://doi.org/10.1016/j.envpol.2019.113428, 2020.

Zheng, J. Y., Yin, S. S., Kang, D. W., Che, W. W., and Zhong, L. J.: Development and uncertainty analysis of a high-resolution NH_3 emissions inventory and its implications with precipitation over the Pearl River Delta region, China, Atmos. Chem. Phys., 12, 7041-7058, https://doi.org/10.5194/acp-12-7041-2012, 2012.

Zong, Z., Tan, Y., Wang, X., Tian, C., Li, J., Fang, Y., Chen, Y., Cui, S., and Zhang, G.: Dual-modelling-based source apportionment of NOx in five Chinese megacities: providing the isotopic footprint from 2013 to 2014, Environ. Int., 137, 105592, https://doi.org/10.1016/j.envint.2020.105592, 2020.

Zong, Z., Wang, X., Tian, C., Chen, Y., Fang, Y., Zhang, F., Li, C., Sun, J., Li, J., and Zhang, G.: First assessment of NOx sources at a regional background site in North China using isotopic analysis linked with modeling, Environ. Sci. Technol., 51, 5923-5931, https://doi.org/10.1021/acs.est.6b06316, 2017.